High-dimensional immune phenotyping of blood cells by mass cytometry in patients infected with hepatitis C virus

Jacobus Herderschee[1], Tytti Heinonen[1], Craig Fenwick[2], Irene T. Schrijver[1], Khalid Ohmiti[2], Darius Moradpour[3], Matthias Cavassini[1], Giuseppe Pantaleo[2,4], Thierry Roger[1$], Thierry Calandra[1$#], and the Swiss HIV Cohort Study

[1]Infectious Diseases Service, [2]Division of Immunology and Allergy, and [3]Division of Gastroenterology and Hepatology, Department of Medicine, Lausanne University Hospital and University of Lausanne, Lausanne; [4]Swiss Vaccine Research Institute, Lausanne, Switzerland.

[$]These authors contributed equally to this work.

[#]Corresponding author: Thierry Calandra. Infectious Diseases Service, Department of Medicine, BH-10.555, Lausanne University Hospital, Rue du Bugnon 46, CH-1011 Lausanne, Switzerland. Thierry.Calandra@chuv.ch Tel: + 41 21 314 10 10; Fax: + 41 21 314 05 97

Length of your abstract: 250 words

Length of the paper (Introduction, Methods, Results, Discussion): 2477 words

Abstract

Objectives

Chronic hepatitis C virus (HCV) infection affects the immune system. Whether elimination of HCV with direct-acting antivirals (DAA) restores immunity is unclear. We used mass cytometry to get a broad and in-depth assessment of blood cell populations of patients with chronic HCV prior to and after DAA therapy.

Methods

Before and 12 weeks after sustained virological response to DAA therapy (SVR12), 22 cell populations were analysed by mass cytometry in blood collected from 10 healthy controls and 20 HCV patients with (10) or without human immunodeficiency virus (HIV) (10) infection.

Results

HCV infection altered the frequency of 14/22 (64%) blood cell populations. At baseline, the frequencies (median [IQR]; control, HCV, HCV/HIV) of intermediate monocytes (1.2 [0.47-1.46], 1.76 [0.83-2.66], 0.78 [0.28-1.77]), non-classical monocytes (1.11 [0.49-1.26], 0.9 [0.18-0.99], 0.54 [0.28-1.77]), conventional dendritic cells type 2 (0.55 [0.35-0.59], 0.31 [0.16-0.38], 0.19 [0.11-0.36]) and $CD56^{dim}$ natural killer cells (8.08 [5.34-9.79], 4.72 [2.59-6.05], 3.61 [2.98-5.07]) were reduced by 35% to 65%, particularly in HCV/HIV co-infected patients. In contrast, activated double-negative T cells (0.07 [0.06-0.10], 0.10 [0.09-0.19], 0.19 [0.12-0.25]), activated CD4 T cells (0.28 [0.21-0.36], 0.56 [0.33-0.77], 0.40 [0.22-0.53]) and activated CD8 T cells (0.23 [0.14-0.42], 0.74 [0.30-1.65], 0.80 [0.58-1.16]) were increased 1.4 to 3.5 times. Upon stimulation with Toll-like receptor ligands, the expression of cytokines was up-regulated in 7/9 (78%) and 17/19 (89%) of the conditions in HCV and HCV/HIV patients, respectively. Most alterations persisted at SVR12.

Conclusions

Chronic HCV and HCV/HIV infections induces profound and durable perturbations of innate and adaptive immune homeostasis.

Introduction

Infections with hepatitis C virus (HCV) and human immunodeficiency virus (HIV) are leading causes of morbidity and mortality worldwide [1]. In 2015, a study estimated that 71 million people were chronically infected with HCV. Among the 37.9 million people living with HIV, 2.3 million were coinfected with HCV [1, 2]. Patients with HCV and HIV coinfection have higher mortality rates than patients with HCV or HIV monoinfection [3]. The ability of HIV and HCV to subvert and evade the host immune response explains why the diseases follow a chronic course [4, 5].

HCV evades the host innate immune system efficiently, preventing a successful adaptive immune response, resulting in chronic infection in up to 80% of patients [1, 5]. In infected hepatocytes, HCV proteins inhibit transduction of signals from pattern recognition receptors and cap-dependent mRNA translation, limiting the production of type I interferon (IFN) and other cytokines, thereby preventing the establishment of an antiviral state [6]. After infection, HCV titers rise within days, reach a plateau of 10^5–10^7 IU/mL and decrease after 4 to 8 weeks contemporaneously with the appearance of HCV-specific CD8 T cells [7]. HCV replication results in prolonged antigenic stimulation associated with disappearance of HCV-specific CD4 T cells and exhaustion of CD8 T cell responses [6, 8]. In HCV/HIV coinfected patients, HCV-specific immunity is impaired further by the depletion of CD4 T cells. Depletion of mucosal CD4 T cells also impairs gut barrier function, leading to increased microbial translocation and production of pro-fibrotic cytokines by Kupffer cells [6]. Thus, HIV infection alters the course of HCV disease *via* combined effects on innate and adaptive immunity.

For two decades, studies of the innate immune responses during HCV therapy were hampered by the use of pegylated-IFNα that exerts widespread effects on cellular immune functions. This changed with the introduction of direct-acting antivirals (DAA) for the treatment of hepatitis C. In this study, we used high-dimensional mass cytometry to get a broad and in-depth qualitative and quantitative assessment of blood cells before, during and after DAA-based therapy in patients with chronic hepatitis C with or without HIV coinfection.

Materials and Methods

Subjects

We conducted a longitudinal, non-interventional study in 10 patients with HCV, 10 patients with HCV and HIV (HCV/HIV), and 10 healthy subjects (controls) (Fig. 1, Table S1). Ethical approval was obtained from the Commission cantonale d'éthique de la recherche sur l'être humain, Canton de Vaud, Switzerland (CER-VD, PB_2016-01464). The project was approved by the Scientific Board of the Swiss HIV Cohort Study (SHCS, project number 788). Study participants provided written informed consent. HCV-infected patients received IFNα-free, DAA-based therapy. Depending on the duration of DAA treatment, follow-up ranged from 6 to 9 months. HCV viral loads were measured at baseline, one or two weeks after initiation of treatment, at the end of therapy, and 12 weeks thereafter to determine whether the patient achieved a sustained virologic response (SVR). For immune profiling, blood was collected in heparin tubes at baseline (within 4 weeks prior to the initiation of DAA-based therapy) and 12 weeks after therapy (SVR12) (#1 and #4, Fig. 1a). To avoid bias linked to cell isolation or cryopreservation, blood was immediately either stabilized for frequency analysis or stimulated as described in Supplementary Materials and Methods. Blood was collected once in healthy controls. HCV or HIV viral loads were determined by the clinical laboratory of the Division of Immunology and Allergy of Lausanne University Hospital.

Processing and clustering of CyTOF data

Information about conjugation of antibodies, mass-tag barcoding, sample staining for CyTOF and data analysis are presented in the Supplementary Materials and Methods and Tables S6-8. Samples were acquired on a CyTOF 2 (Fluidigm) [9]. Flow cytometry standard (FCS) files were normalized using the MATLAB normalizer [10]. Debris were gated out manually and barcoded files were deconvoluted using OpenCyto-based boolean gating [11]. FlowSOM clustering was performed on 99.5^{th} percentile scaled, hyperbolic arcsine transformed expression levels, using co-factor 5, for the markers CD1c, CD3, CD4, CD7, CD8, CD11b, CD11c, CD14, CD16, CD20, CD38, CD56, CD66b, CD123, CD141, HLADR and Slan [12]. We overclustered the data to 40 metaclusters, manually merged into 22 populations based on biological knowledge [13]. For dimensionality reduction, we performed Uniform Manifold Approximation Projection (UMAP) with a minimal distance of 0.2 on a dataset down-sampled to 5000 randomly selected cells per sample [14].

Statistical analysis

Data were analyzed in R with the lme4 package using generalized linear mixed models [13]. To control for batch effects, random effects were added for sample and batch. Thresholds for cytokine positivity were determined as the 99th percentile levels of matched unstimulated samples that were processed simultaneously and identically as stimulated sample in a subject and time point dependent fashion [15]. Median signal intensities (MSI) of cytokines and co-stimulatory or inhibitory markers were calculated and compared with linear models. For all methods, *p* values were extracted and corrected for multiple testing using the false discovery rate (FDR). We used a threshold of 5% to indicate statistical significance and of 15% to indicate a trend. Only FDR adjusted *p* values are shown. Statements regarding percentage increase or decrease are based on medians. For boxplots show the 75th and 25th percentile, the horizontal line the median and the whiskers hinges to 1.5-times the interquartile range. Heatmaps show normalized frequencies where the frequency of each population is scaled 0-1.

Results

Characteristics of patients and controls

We conducted a longitudinal, non-interventional study in 10 patients infected with HCV, 10 patients infected with HCV and HIV (HCV/HIV), and 10 healthy subjects (controls) (Fig.1a and Table S1). Patients and controls were recruited by the Infectious Diseases Service and Division of Gastroenterology and Hepatology of Lausanne University Hospital (Switzerland). HCV patients were slightly older than controls (p=0.001) and HCV/HIV patients (p=0.042). Baseline HCV loads and viral load reductions were comparable in HCV and HCV/HIV patients. All subjects achieved sustained virologic response 12 weeks after the end of therapy and completed the follow-up period (Fig. 1b). Whole blood was collected from healthy controls and patients just before, during and after DAA therapy and used immediately to perform in-depth immunoprofiling (Fig. 1a).

HCV infection causes extensive and sustained changes in populations of circulating immune cells

Twenty-two cell populations were identified in whole blood by mass cytometry and FlowSOM clustering (Fig. 1c,d, Figs S1-S3). It included 3 granulocyte clusters (basophils, $CD11b^{high}$ and $CD11b^{low}$ neutrophils), intermediate and non-classical monocytes, type 2 conventional DCs (cDC2), plasmacytoid DCs (pDCs), classical, $CD56^{high}$ and $CD56^{dim}$ NK cells, $CD1c^{+}$, $CD11c^{+}$ and $CD1c^{-}$/$CD11c^{-}$ B cells, CD4 and CD8 double-negative (DN), single-positive (SP) and double-positive (DP) T cells. T cell subsets included activated and non-activated T cells according to CD38 and HLA-DR expression.

We compared the frequency of merged clusters at baseline in controls and patients using generalized mixed linear models [13]. The full dataset of the normalized frequencies of immune cell populations prior to antiviral therapy and at SVR12 is shown in Fig. 2a. The proportion of the main subsets of innate and adaptive immune cells is reported in Table S2 and Table S3. Overall, both HCV monoinfection and HCV/HIV coinfection were associated with significant changes in the frequency of 14 of 22 (64%) immune cell populations (Fig. 2b). Prior to therapy, innate immune cells were markedly reduced. The reduction was 35% to 51% for intermediate and non-classical monocytes (HCV/HIV, p=0.038), 44% to 65% for cDC2 (HCV, p=0.007; HCV/HIV, p<0.001) and 42% to 55% for circulating $CD56^{dim}$ NK cells (HCV, p=0.074; HCV/HIV, p=0.012). In contrast, the frequencies of activated DN T cells (HCV, p=0.042; HCV/HIV, p<0.001), activated CD4 T cells (HCV, p=0.059), CD8 T cells (HCV/HIV, p<0.001) and activated CD8 T cells (HCV, p=0.023; HCV/HIV, p=0.025) were increased by a factor ranging from 1.4 to 3.5. The frequencies of B cells and

CD11c$^+$ B cells were increased 2.1 and 3-fold in HCV/HIV coinfected patients (p=0.125 and p=0.042). Except for cDC2 (HCV patients) and activated DN cells (HCV and HCV/HIV patients), changes in innate and adaptive cell populations persisted up to SVR12 (Figs 2 and 3). Consistent with this observation, SVR12 samples tended to cluster with baseline samples from the same group.

Impact of HCV infection on innate immune responses

To investigate the effect of HCV on innate immune function, we stimulated whole blood with TLR agonists (LPS and R848) and analysed the expression of pro-inflammatory (TNF, IL-1α, IL-1β, IL-6, IL-8, IL-12p40, IFNα and MCP-1) and anti-inflammatory (IL-1RA and IL-10) cytokines by mass cytometry (Figs S4-S9). The full dataset of cytokine expression is shown in Fig. 4a, Fig. 5, Table S4 and Table S5. Cytokine expression induced by LPS and R848 clustered by cell type (Fig. 4a). Classical, intermediate and non-classical monocytes and cDC2 had the highest frequencies of TNF, IL-1α, IL-1β and IL-8-positive cells after LPS stimulation. All classes of innate immune cells had a high frequency of TNF-positive cells after R848 stimulation, while cDC2, classical, intermediate and non-classical monocytes had the highest frequencies of IL-1β and IL-8-positive cells and pDCs had the highest frequency of IFNα-positive cells. Overall, the frequency of TNF, IL-1α, IL-1β, IL-6 and IL-8 cytokine-positive cells was higher in classical, intermediate and non-classical monocytes especially in HCV/HIV patients after stimulation with R848 (Fig. 4b)**.** The trend was less striking in cDC2. The frequency of IFNα-positive cells was also higher in HCV/HIV patients than in controls. In contrast, the expression of IL-1RA and IL-10 by monocytes and DCs did not differ between patients and controls. The pro-inflammatory signature of monocytes persisted up to SVR12 in HCV/HIV patients and to a lesser degree in HCV patients (Fig. 5).

Inflammatory signals enhance the expression of CD80 and CD86 co-stimulatory molecules and PD-1 and PD-L1 immune checkpoint molecules by antigen presenting cells [16]. Considering the pro-inflammatory signature of HCV patients, we analysed the expression CD80, CD86, PD-1 and PD-L1 by monocytes, cDC2 and pDCs. At baseline or 24 hours after LPS stimulation, we found no differences in the expression of these molecules by innate immune cells of patients and controls (cDC2 are shown in Fig. S10).

Discussion

Patients infected with HCV with or without HIV display an immune signature characterized by altered innate and adaptive immune cell profiles and cytokine response by monocytes and DCs. Innate immunity was severely dysregulated. Chronic HCV caused a profound and widespread decrease of intermediate and non-classical monocytes, cDC2 and $CD56^{dim}$ NK cells. Yet, *ex vivo* production of pro-inflammatory cytokines by innate immune cells was upregulated particularly in HCV/HIV patients. Adaptive immune signatures were upregulated, with increased frequencies of activated DN, CD4, and CD8 T lymphocytes. This HCV-related immune dysregulation persisted up to 12 weeks after HCV clearance.

Previous studies on the effects of HCV used fresh or cryopreserved peripheral blood mononuclear cells (PBMCs) or monocyte-derived DCs (moDCs) and a limited number of phenotypic markers [17-25]. Isolation, cryopreservation and differentiation alter the phenotype and function of PBMCs and moDCs. To avoid these limitations, we analysed blood immediately after drawing and mass cytometry with clustering strategies allowing the identification of a broad spectrum of immune cells and cytokines. Studies of innate immunity in HCV patients yielded mixed results. Some studies reported a clear reduction in the frequency and function of pDCs and cDCs, while others did not [17-24, 26]. Our results are unambiguous with striking reduction of intermediate and non-classical monocytes, cDC2 and $CD56^{dim}$ NK cells. The broad and persistent reduction in circulating innate immune cells is an important hallmark of acute hepatitis C and possibly part of a strategy whereby HCV evades innate immune responses and prevents the development of an effective adaptive immune response. HCV-infected patients do not suffer from opportunistic infections, nor do they appear to be protected against other infections. The response to vaccination, such as against HBV, appears to be intact in patients with HCV infection, although some authors have found a reduced response [27].

Cytokine analysis at the single cell level revealed a pro-inflammatory profile in patients. One cannot exclude a restoration of immune homeostasis beyond SVR12. However, the persistence of immune alterations may be a systemic signature consistent with reports of ongoing liver inflammation documented long after SVR in patients with normal levels of transaminases [28-30]. If sustained, the inflammatory signature may contribute to the development of HCV-associated complications such as hepatocellular carcinoma, cardiovascular disease and diabetes. Along this line, increased cytokine response by innate immune cells were more pronounced in HCV/HIV patients than in HCV patients, indicating that HIV

coinfection amplified immunophenotypic alterations. This observation may explain the progression of liver disease, including cirrhosis, liver failure and hepatocellular carcinoma in HCV/HIV patients. Of note, coinfected patients had HIV viral loads below the lower limit of detection. Coinfected patients receiving HIV treatment progress more slowly than untreated patients. Yet, disease progression in the context of an undetectable HIV viral load remains incompletely understood [6].

HCV infection has been associated with broad-spectrum alterations of adaptive immunity [5]. We confirmed and extended these findings by demonstrating increased frequencies of activated DN T cells at baseline that normalized after viral clearance. We also observed an increase in activated CD8 T cells in HCV and HCV/HIV at baseline that persisted up to SVR12. A recent study reported a molecular signature of exhaustion that persisted in HCV-specific CD8 T cells after DAA-mediated cure of HCV [8]. This illustrates the strength of the clustering approach to look at a broad range of cell populations. As we did not examine antigen specificity of T cells, we did not check for T cell exhaustion in chronically infected patients. We cannot differentiate between the expansion of HCV-specific T cells driven by the high HCV mutation rate or the expansion of non-HCV-specific T cells linked to a general pro-inflammatory status or secondary to other patient characteristics such as fibrosis. Chronic hepatitis C is characterized by an increased risk of progressive liver fibrosis and immune complex-mediated autoimmunity [1]. The increased frequencies of activated T cells in patients with chronic HCV infection may facilitate the development of these features.

Our study has several strengths and limitations. We performed whole blood analysis of 22 cell populations and conducted *ex vivo* functional studies by mass cytometry in patients before, during and up to 12 weeks after DAA-mediated virological cure. The limited number of subjects may have limited our ability to detect more subtle changes possibly linked to HCV genotype or host genetic or risk factors features. An HIV mono-infected group could have been included. Finally, all patients were under ART and had low or undetectable HIV viral loads, precluding to detect interactions between HIV with HCV infections.

High-dimensional immune profiling of blood cells provided a broad and in-depth picture of the systemic immune dysregulation induced by chronic HCV. A salient finding was the observation of a profound derangement of the homeostasis of the immune system triggered by HCV characterized by a pro-inflammatory innate immune signature extending well beyond the clearance of HCV, especially in HCV/HIV

patients. This inflammatory phenotype may contribute to the pathogenesis of systemic complications of chronic HCV infection.

Acknowledgments

The authors gratefully acknowledge the expert study support by Adeline Mathieu, Maribelle Herranz and Deolinda Alves. The authors also thank Prof. Christine Sempoux for helpful discussions on the topic of persistent inflammation in liver biopsies after SVR. This work was supported by grants from the Swiss National Science Foundation (SNSF) grant number CRSII3_147662S to TC and GP, 310030_173123 to TR, and 177499 to the Swiss HIV Cohort Study, and by the European Sepsis Academy Horizon 2020 Marie Skłodowska-Curie Action: Innovative Training Network (MSCA-ESA-ITN) grant number 676129 to TR and TC. TH and ITS received a scholarship from the Société Académique Vaudoise (Lausanne, Switzerland).

Author contributions statement

JH, TR and TC designed the study. MC and DM recruited the patients. JH, TH and IS processed the blood samples. CF and GP gave advice and access to the CyTOF. JH performed CyTOF studies. JH and KO performed computational analysis of the data. JH, TR and TC analysed and interpreted the data. JH, TR and TC wrote the manuscript. All the authors revised the manuscript.

Members of the Swiss HIV Cohort Study

Aebi-Popp K, Anagnostopoulos A, Battegay M, Bernasconi E, Böni J, Braun DL, Bucher HC, Calmy A, Cavassini M, Ciuffi A, Dollenmaier G, Egger M, Elzi L, Fehr J, Fellay J, Furrer H, Fux CA, Günthard HF (President of the SHCS), Haerry D (deputy of "Positive Council"), Hasse B, Hirsch HH, Hoffmann M, Hösli I, Huber M, Kahlert CR (Chairman of the Mother & Child Substudy), Kaiser L, Keiser O, Klimkait T, Kouyos RD, Kovari H, Ledergerber B, Martinetti G, Martinez de Tejada B, Marzolini C, Metzner KJ, Müller N, Nicca D, Paioni P, Pantaleo G, Perreau M, Rauch A (Chairman of the Scientific Board), Rudin C, Scherrer AU (Head of Data Centre), Schmid P, Speck R, Stöckle M (Chairman of the Clinical and Laboratory Committee), Tarr P, Trkola A, Vernazza P, Wandeler G, Weber R, Yerly S.

Conflict of Interest Statement

The authors do not have any conflict of interest regarding this manuscript.

References

[1] Spearman CW, Dusheiko GM, Hellard M ,Sonderup M. Hepatitis C. Lancet **2019**; 394:1451-1466.

[2] Collaborators POH. Global prevalence and genotype distribution of hepatitis C virus infection in 2015: a modelling study. Lancet Gastroenterol Hepatol **2017**; 2:161-176.

[3] Chen TY, Ding EL, Seage III GR ,Kim AY. Meta-analysis: increased mortality associated with hepatitis C in HIV-infected persons is unrelated to HIV disease progression. Clin Infect Dis **2009**; 49:1605-15.

[4] Fenwick C, Joo V, Jacquier P, Noto A, Banga R, Perreau M, et al. T-cell exhaustion in HIV infection. Immunol Rev **2019**; 292:149-163.

[5] Shin EC, Sung PS ,Park SH. Immune responses and immunopathology in acute and chronic viral hepatitis. Nat Rev Immunol **2016**; 16:509-23.

[6] Chen JY, Feeney ER ,Chung RT. HCV and HIV co-infection: mechanisms and management. Nat Rev Gastroenterol Hepatol **2014**; 11:362-71.

[7] Shin EC, Park SH, Demino M, Nascimbeni M, Mihalik K, Major M, et al. Delayed induction, not impaired recruitment, of specific CD8(+) T cells causes the late onset of acute hepatitis C. Gastroenterology **2011**; 141:686-95, 695 e1.

[8] Hensel N, Gu Z, Sagar, Wieland D, Jechow K, Kemming J, et al. Memory-like HCV-specific CD8(+) T cells retain a molecular scar after cure of chronic HCV infection. Nat Immunol **2021**; 22:229-239.

[9] Ciarlo E, Heinonen T, Herderschee J, Fenwick C, Mombelli M, Le Roy D, et al. Impact of the microbial derived short chain fatty acid propionate on host susceptibility to bacterial and fungal infections in vivo. Sci Rep **2016**; 6:37944.

[10] Finck R, Simonds EF, Jager A, Krishnaswamy S, Sachs K, Fantl W, et al. Normalization of mass cytometry data with bead standards. Cytometry A **2013**; 83:483-94.

[11] Finak G, Frelinger J, Jiang W, Newell EW, Ramey J, Davis MM, et al. OpenCyto: an open source infrastructure for scalable, robust, reproducible, and automated, end-to-end flow cytometry data analysis. PLoS Comput Biol **2014**; 10:e1003806.

[12] Van Gassen S, Callebaut B, Van Helden MJ, Lambrecht BN, Demeester P, Dhaene T, et al. FlowSOM: Using self-organizing maps for visualization and interpretation of cytometry data. Cytometry A **2015**; 87:636-45.

[13] Nowicka M, Krieg C, Weber LM, Hartmann FJ, Guglietta S, Becher B, et al. CyTOF workflow: differential discovery in high-throughput high-dimensional cytometry datasets. F1000Res **2017**; 6:748.

[14] Becht E, McInnes L, Healy J, Dutertre C-A, Kwok IWH, Ng LG, et al. Dimensionality reduction for visualizing single-cell data using UMAP. Nature Biotechnology **2019**; 37:38-44.

[15] Newell EW, Sigal N, Bendall SC, Nolan GP ,Davis MM. Cytometry by time-of-flight shows combinatorial cytokine expression and virus-specific cell niches within a continuum of CD8+ T cell phenotypes. Immunity **2012**; 36:142-52.

[16] Chen L, Flies DB. Molecular mechanisms of T cell co-stimulation and co-inhibition. Nat Rev Immunol **2013**; 13:227-42.

[17] Auffermann-Gretzinger S, Keeffe EB ,Levy S. Impaired dendritic cell maturation in patients with chronic, but not resolved, hepatitis C virus infection. Blood **2001**; 97:3171-6.

[18] Barnes E, Salio M, Cerundolo V, Francesco L, Pardoll D, Klenerman P, et al. Monocyte derived dendritic cells retain their functional capacity in patients following infection with hepatitis C virus. J Viral Hepat **2008**; 15:219-28.

[19] Cicinnati VR, Kang J, Sotiropoulos GC, Hilgard P, Frilling A, Broelsch CE, et al. Altered chemotactic response of myeloid and plasmacytoid dendritic cells from patients with chronic hepatitis C: role of alpha interferon. J Gen Virol **2008**; 89:1243-53.

[20] Dolganiuc A, Chang S, Kodys K, Mandrekar P, Bakis G, Cormier M, et al. Hepatitis C virus (HCV) core protein-induced, monocyte-mediated mechanisms of reduced IFN-alpha and plasmacytoid dendritic cell loss in chronic HCV infection. J Immunol **2006**; 177:6758-68.

[21] Gelderblom HC, Nijhuis LE, de Jong EC, te Velde AA, Pajkrt D, Reesink HW, et al. Monocyte-derived dendritic cells from chronic HCV patients are not infected but show an immature phenotype and aberrant cytokine profile. Liver Int **2007**; 27:944-53.

[22] Kakumu S, Ito S, Ishikawa T, Mita Y, Tagaya T, Fukuzawa Y, et al. Decreased function of peripheral blood dendritic cells in patients with hepatocellular carcinoma with hepatitis B and C virus infection. J Gastroenterol Hepatol **2000**; 15:431-6.

[23] Kanto T, Hayashi N, Takehara T, Tatsumi T, Kuzushita N, Ito A, et al. Impaired allostimulatory capacity of peripheral blood dendritic cells recovered from hepatitis C virus-infected individuals. J Immunol **1999**; 162:5584-91.

[24] Longman RS, Talal AH, Jacobson IM, Albert ML ,Rice CM. Presence of functional dendritic cells in patients chronically infected with hepatitis C virus. Blood **2004**; 103:1026-9.

[25] Vita S, Zuccala P, Savinelli S, Mascia C, Rossi R, Schiavone F, et al. Impact of IFN-free and IFN-based treatment on blood myeloid dendritic cell, monocyte, slan-DC, and activated T lymphocyte dynamics during HCV infection. J Immunol Res **2020**; 2020:2781350.

[26] Judge CJ, Kostadinova L, Sherman KE, Butt AA, Falck-Ytter Y, Funderburg NT, et al. CD56(bright) NK IL-7Ralpha expression negatively associates with HCV level, and IL-7-induced NK function is impaired during HCV and HIV infections. J Leukoc Biol **2017**; 102:171-184.

[27] Liu J, Wu H ,Chen H. Immune response to hepatitis B vaccine in patients with chronic hepatitis C infection: A systematic review and meta-analysis. Hepatol Res **2018**; 48:119-126.

[28] Welsch C, Efinger M, von Wagner M, Herrmann E, Zeuzem S, Welzel TM, et al. Ongoing liver inflammation in patients with chronic hepatitis C and sustained virological response. PLoS One **2017**; 12:e0171755.

[29] Putra J, Schiano TD ,Fiel MI. Histological assessment of the liver explant in transplanted hepatitis C virus patients achieving sustained virological response with direct-acting antiviral agents. Histopathology **2018**; 72:990-996.

[30] Amaddeo G, Nguyen CT, Maille P, Mule S, Luciani A, Machou C, et al. Intrahepatic immune changes after hepatitis c virus eradication by direct-acting antiviral therapy. Liver Int **2020**; 40:74-82.

Fig. 1. Study design, HCV viral loads and analyses of blood cell populations with mass cytometry workflow. (a) Blood samples were obtained within 4 weeks of the start of therapy (baseline, #1), after 1 week of treatment (#2), at the end of treatment (#3), and 12 weeks after the end treatment and sustained virologic response (SVR12) (#4). Four blood samples (#1 to 4) were collected for measurement of HCV viral loads and two blood samples (#1 and #4) were collected for immune profiling. **(b)** HCV viral loads. Each dot represents one single patient (some dots overlap). The solid line connects the median viral loads of each time point. RNA levels were similar in patients with HCV or HCV/HIV infections. The horizontal dotted line indicates the lower limit of detection of the test (15 IU/ml). **(c)** Heatmap showing expression of markers and blood cell populations. Each row corresponds to a manually annotated immune cell type based on the profile identified with the markers (columns) used for clustering. Data are expressed as median of hyperbolic arcsine transformed signal intensities (MSI). **(d)** Dimensionality reduction with UMAP performed with a random subset of 5000 cells per sample. Colors correspond to merged and annotated FlowSOM clusters (populations).

Fig. 2. Changes of immune cell populations in patients infected with HCV or HCV and HIV. (a) Heatmap showing normalized frequencies of cell subsets in unstimulated samples at baseline and at SVR12. The scale of normalized frequencies ranges from 0 to 1. Row order was determined by hierarchical clustering. The group and timepoint column serve as a legend and was not used for clustering. **(b)** Summary of statistically significant changes in immune cell populations observed at baseline and at SVR12 when compared to healthy controls (N=10 in each group). Red, white and blue squares show increased, unchanged or decreased frequencies of the immune cell populations shown on the y-axis. Numbers in cells indicate fold-change and p value (in brackets). Medians of the frequency of cytokine positive cells and p values are provided in Tables S2 and S3.

Fig. 3. Proportions of innate and adaptive immune cells before and after HCV therapy. Box plots of the frequencies of intermediate monocytes, type 2 conventional DC (cDC2) and $CD56^{dim}$ NK cells **(a)** and activated double negative (DN) T cells, activated CD4 T cells and activated CD8 T cells **(b)** at baseline and at SVR12. N=10 in each group. Each dot represents one individual subject. Statistical analyses were

performed using mixed linear models. P values corrected for multiple testing using the false discovery rate are provided in Tables S2 and S3.

Fig. 4. Cytokine response of innate immune cells in patients infected with HCV or HCV and HIV. (a) Frequency of cytokine-positive innate immune cells following stimulation with LPS or R848 of blood samples collected at baseline and SVR12. Row order was determined by hierarchical clustering. Left two columns serve as a legend and have not been used for clustering. **(b)** Summary of statistically significant changes in the frequency of cytokine-positive innate immune cells at baseline and at SVR12 when compared to healthy controls (N=10 in each group). Red, white and blue squares illustrate increased, unchanged or decreased frequencies. Numbers in each cell indicate fold-change and p value (in brackets). Medians of the frequency of cytokine positive cells and p values are provided in Tables S4 and S5.

Fig. 5. Proportion of cytokine-positive classical monocytes after stimulation with a TLR7/8 agonist. Box plots of the frequencies of classical monocytes positive for IL-1α, IL-1β, IL-6 and IL-8 after stimulation with R848 at baseline and at SVR12. N=10 in each group. Statistical analysis was performed using mixed linear models. P values corrected for multiple testing using the false discovery rate are provided in Tables S4 and S5.

Graphical abstract

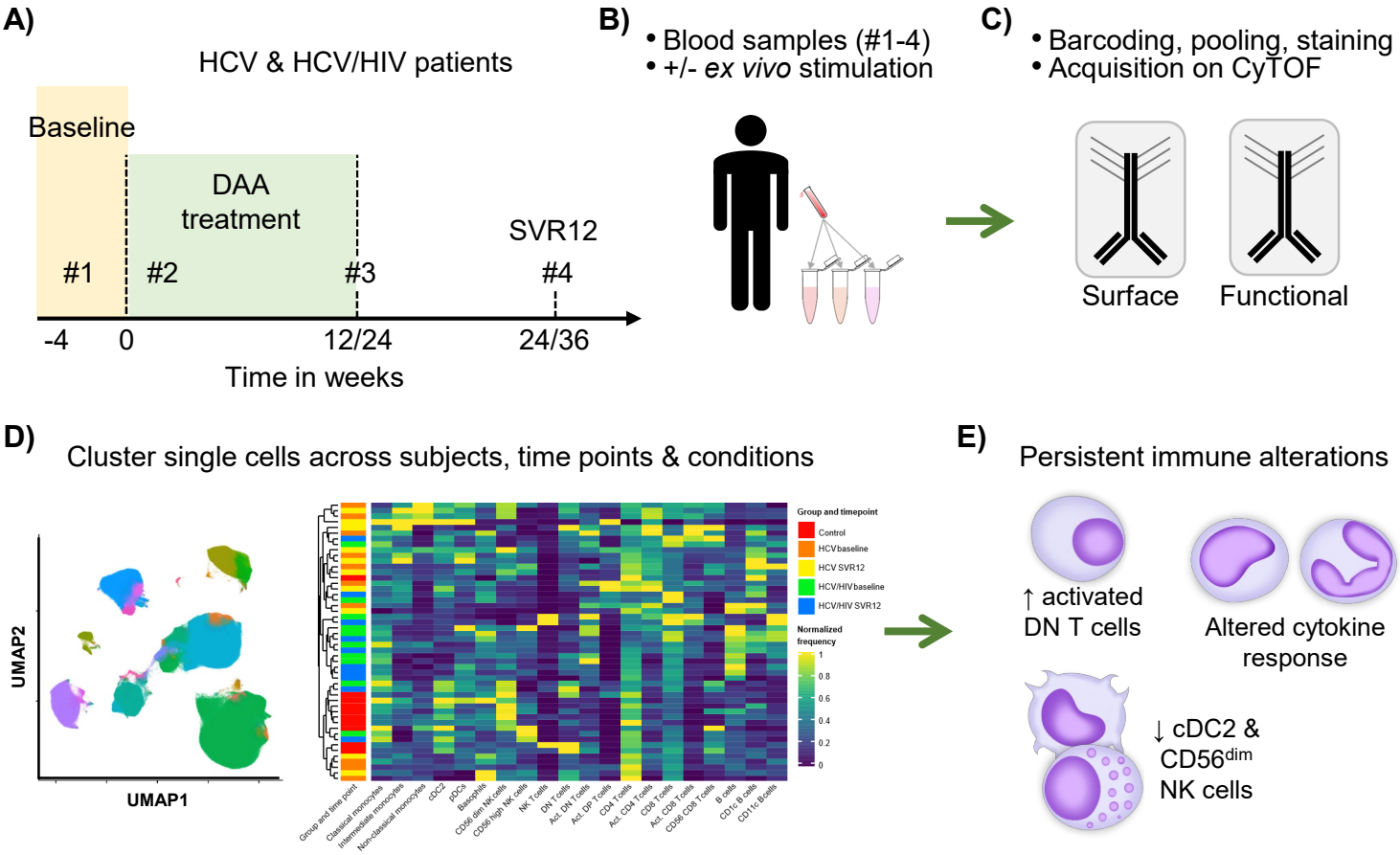

Fig. 1

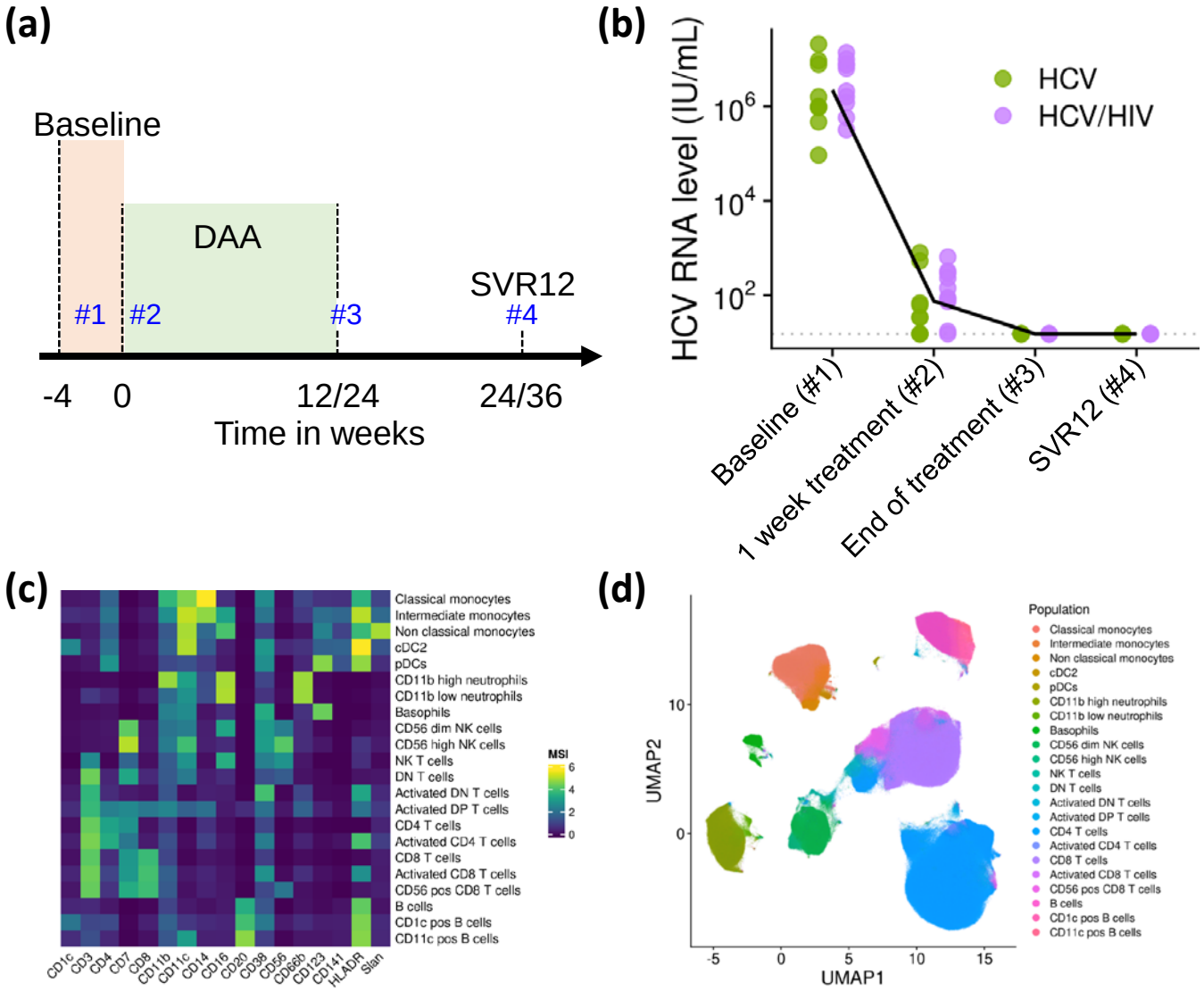
(a)
Baseline
DAA
SVR12
#1
#2
#3
#4
-4
0
12/24
24/36
Time in weeks
(b)
HCV RNA level (IU/mL)
10^6
10^4
10^2
HCV
HCV/HIV
Baseline (#1)
1 week treatment (#2)
End of treatment (#3)
SVR12 (#4)
(c)
Classical monocytes
Intermediate monocytes
Non classical monocytes
cDC2
pDCs
CD11b high neutrophils
CD11b low neutrophils
Basophils
CD56 dim NK cells
CD56 high NK cells
NK T cells
DN T cells
Activated DN T cells
Activated DP T cells
CD4 T cells
Activated CD4 T cells
CD8 T cells
Activated CD8 T cells
CD56 pos CD8 T cells
B cells
CD1c pos B cells
CD11c pos B cells
MSI
6
4
2
0
CD1c
CD3
CD4
CD7
CD8
CD11b
CD11c
CD14
CD16
CD20
CD38
CD56
CD66b
CD123
CD141
HLADR
Slan
(d)
UMAP2
10
0
-5
0
5
10
15
UMAP1
Population
Classical monocytes
Intermediate monocytes
Non classical monocytes
cDC2
pDCs
CD11b high neutrophils
CD11b low neutrophils
Basophils
CD56 dim NK cells
CD56 high NK cells
NK T cells
DN T cells
Activated DN T cells
Activated DP T cells
CD4 T cells
Activated CD4 T cells
CD8 T cells
Activated CD8 T cells
CD56 pos CD8 T cells
B cells
CD1c pos B cells
CD11c pos B cells

Fig. 2

(a)

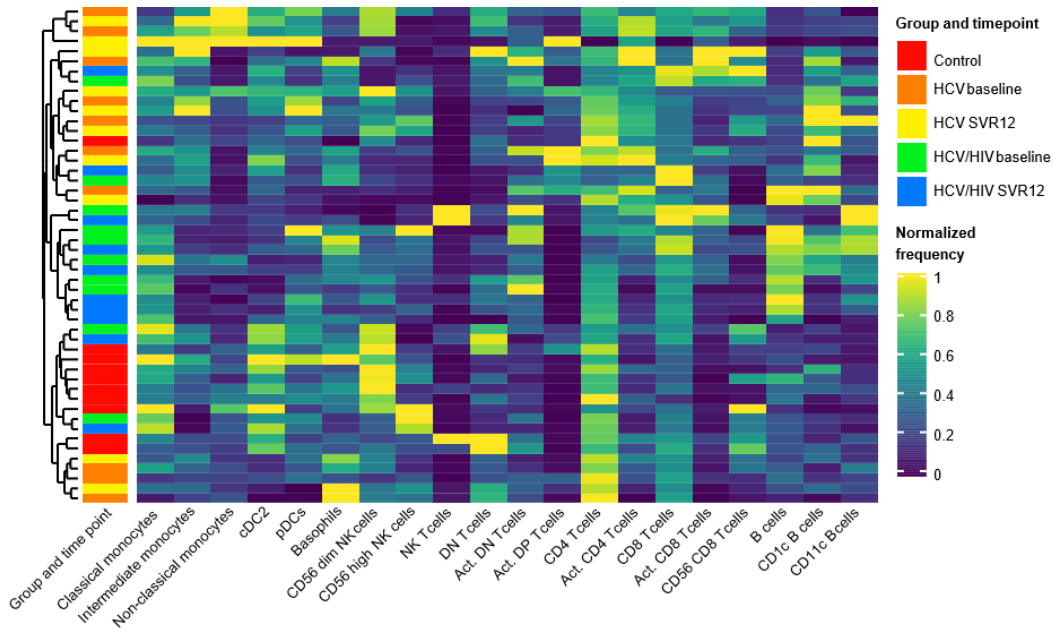

(b)

		HCV		HCV/HIV	
		Baseline	SVR12	Baseline	SVR12
Innate immunity	Intermediate monocytes		2.0 (0.076)	0.65 (0.038)	0.78 (0.126)
	Non-classical monocytes			0.49 (0.038)	0.40 (0.019)
	cDC2	0.56 (0.007)		0.35 (< 0.001)	0.51 (0.041)
	$CD56^{dim}$ NK cells	0.58 (0.074)	0.56 (0.146)	0.45 (0.012)	0.44 (0.020)
	$CD56^{high}$ NK cells				0.60 (0.088)
Adaptive immunity	DN T cells				0.62 (0.146)
	Activated DN T cells	1.4 (0.042)		2.7 (<0.001)	
	Activated DP T cells	12.0 (0.004)	11.0 (0.002)		
	CD4 T cells			0.73 (<0.001)	0.82 (<0.015)
	Activated CD4 T cells	2.0 (0.059)	2.0 (0.008)		
	CD8 T cells			1.4 (<0.001)	1.5 (0.001)
	Activated CD8 T cells	3.2 (0.023)	3.0 (0.024)	3.5 (0.025)	1.8 (0.078)
	B cells			2.1 (0.125)	1.8 (0.061)
	CD11c positive B cells			3.0 (0.042)	1.9 (0.061)

Fig. 3

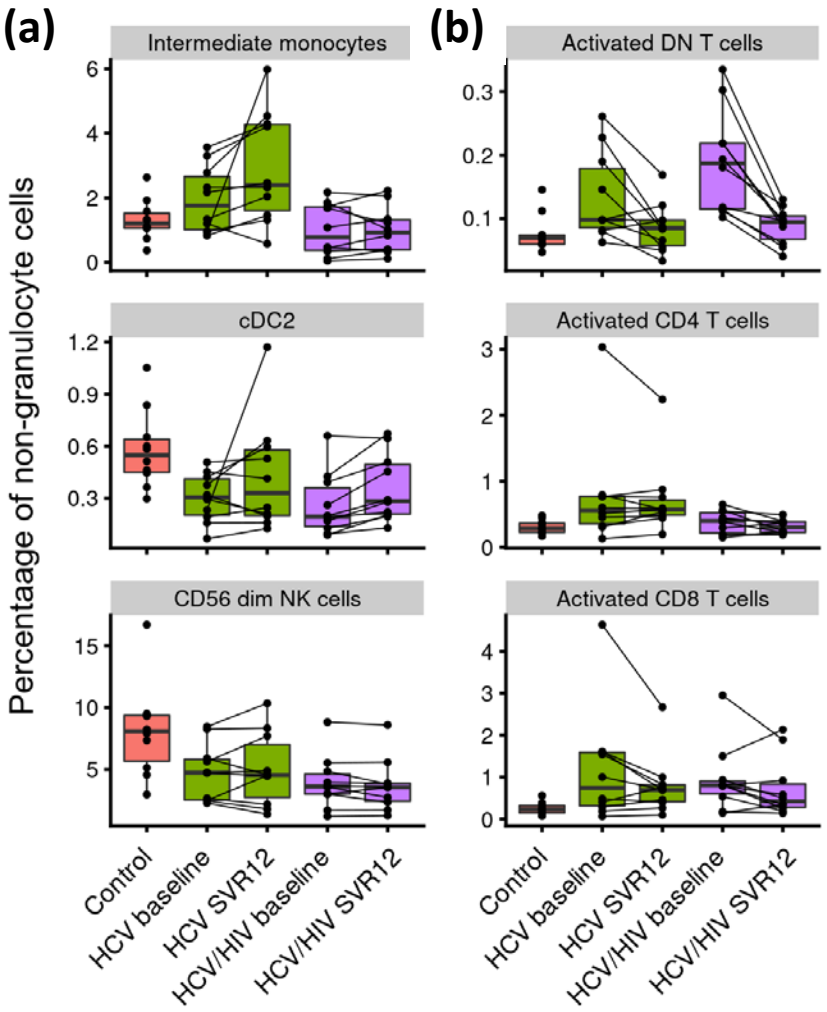
(a)
(b)
Intermediate monocytes
Activated DN T cells
cDC2
Activated CD4 T cells
CD56 dim NK cells
Activated CD8 T cells
Percentaage of non-granulocyte cells
Control
HCV baseline
HCV SVR12
HCV/HIV baseline
HCV/HIV SVR12

Fig. 4

(a)

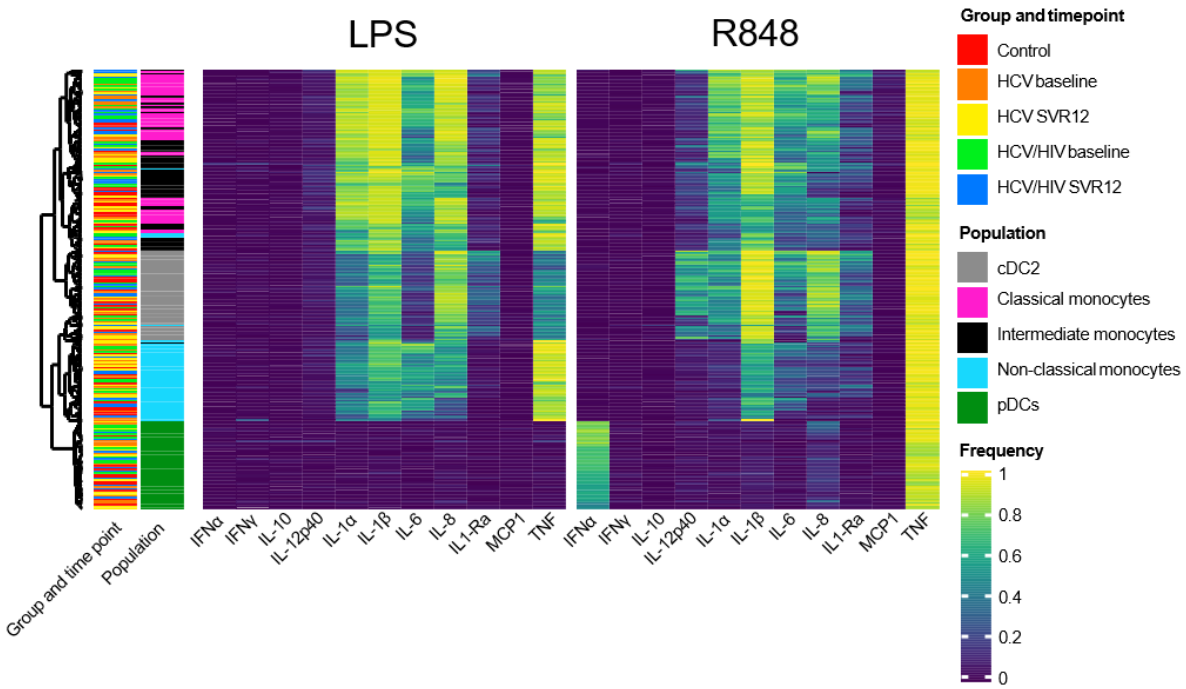

(b)

		LPS				R848			
		HCV		HCV/HIV		HCV		HCV/HIV	
		Baseline	SVR12	Baseline	SVR12	Baseline	SVR12	Baseline	SVR12
Classical monocytes	TNF		0.87 (0.029)		0.94 (0.091)			1.04 (<0.001)	1.06 (<0.001)
	IL-8			1.05 (0.125)	1.04 (0.005)	1.45 (0.016)	1.21 (0.098)	1.42 (0.004)	1.46 (<0.001)
	IL-6							1.52 (<0.001)	1.35 (0.002)
	IL-1β			1.02 (0.004)	1.02 (0.005)	1.26 (0.041)		1.37 (<0.001)	1.09 (0.143)
	IL-1α	0.94 (0.149)	0.95 (0.015)					1.32 (<0.001)	1.23 (0.001)
Intermediate monocytes	TNF							1.01 (0.041)	
	IL-8	1.20 (0.007)	1.25 (0.055)			2.18 (0.001)	2.04 (<0.001)	1.61 (0.021)	1.39 (0.016)
	IL-1β	1.04 (0.071)	1.25 (0.055)					1.11 (0.101)	1.09 (0.143)
	IL-1α					1.49 (0.002)		1.30 (0.038)	1.43 (0.005)
Non-classical monocytes	TNF			1.07 (0.049)				1.10 (0.049)	
	IL-8	1.45 (0.059)	1.65 (0.055)		1.42 (0.143)				
	IL-6							1.10 (0.141)	
cDC2	TNF					0.90 (0.023)	0.98 (0.100)	0.99 (0.005)	
	IL-12p40							0.79 (0.026)	
	IL-6						0.41 (0.143)	1.33 (0.021)	1.26 (0.100)
	IL-1β				1.05 (0.129)		0.96 (0.043)		
	IL-1α						0.91 (0.143)	1.26 (0.031)	1.33 (0.026)
pDC	IFNα							1.20 (0.026)	

Fig. 5

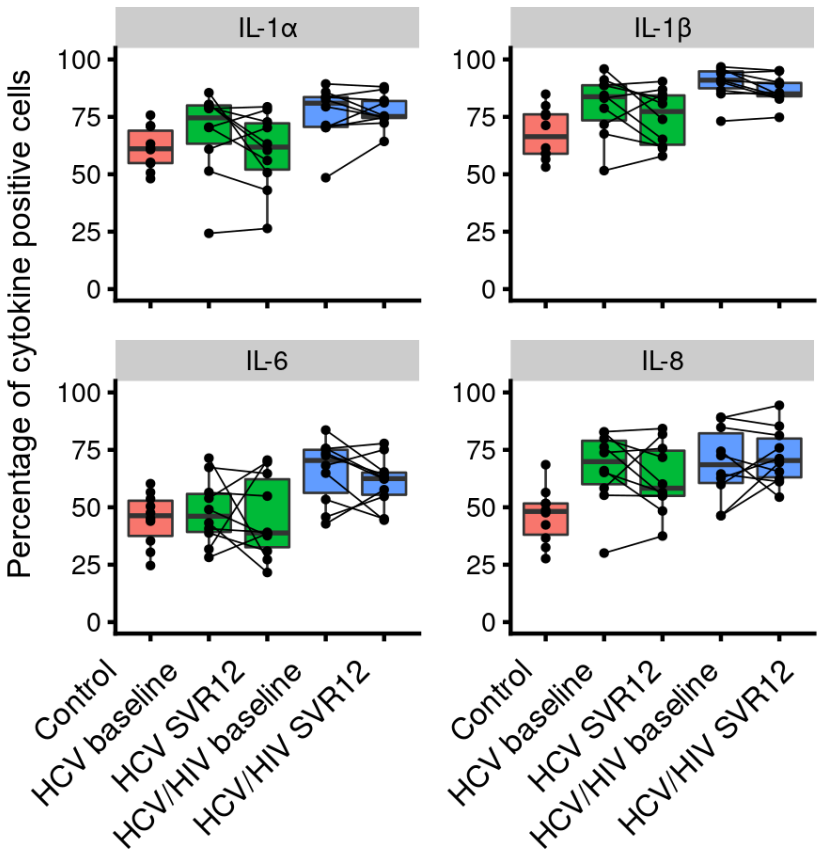
IL-1α
IL-1β
IL-6
IL-8
Percentage of cytokine positive cells
100
75
50
25
0
Control
HCV baseline
HCV SVR12
HCV/HIV baseline
HCV/HIV SVR12

Fig. S1

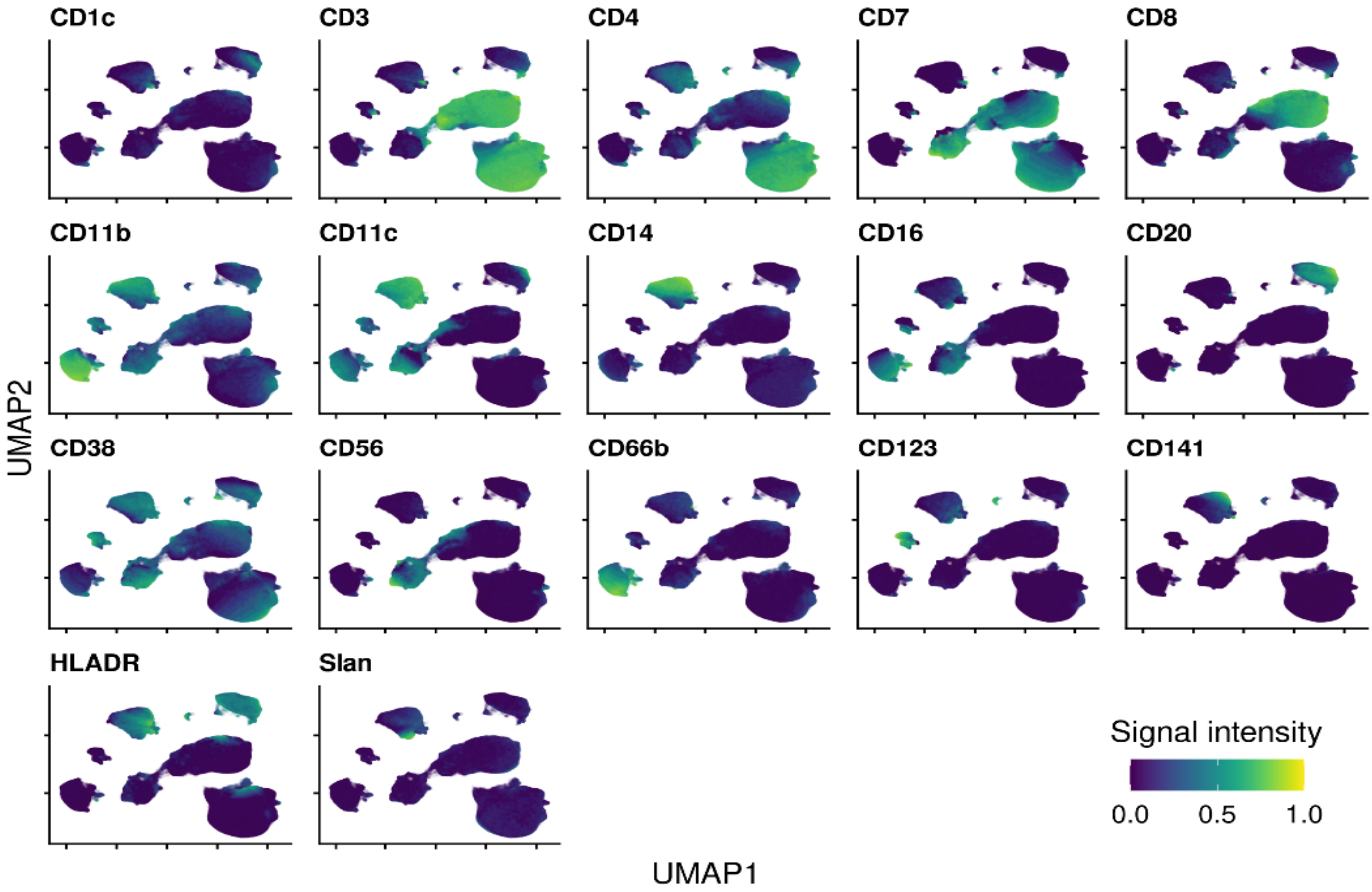

Fig. S1. Analyses of blood cell populations with mass cytometry. Blood samples were analyzed as described in Materials and Methods. UMAP plots show normalized signal intensity of markers used for clustering.

Fig. S2

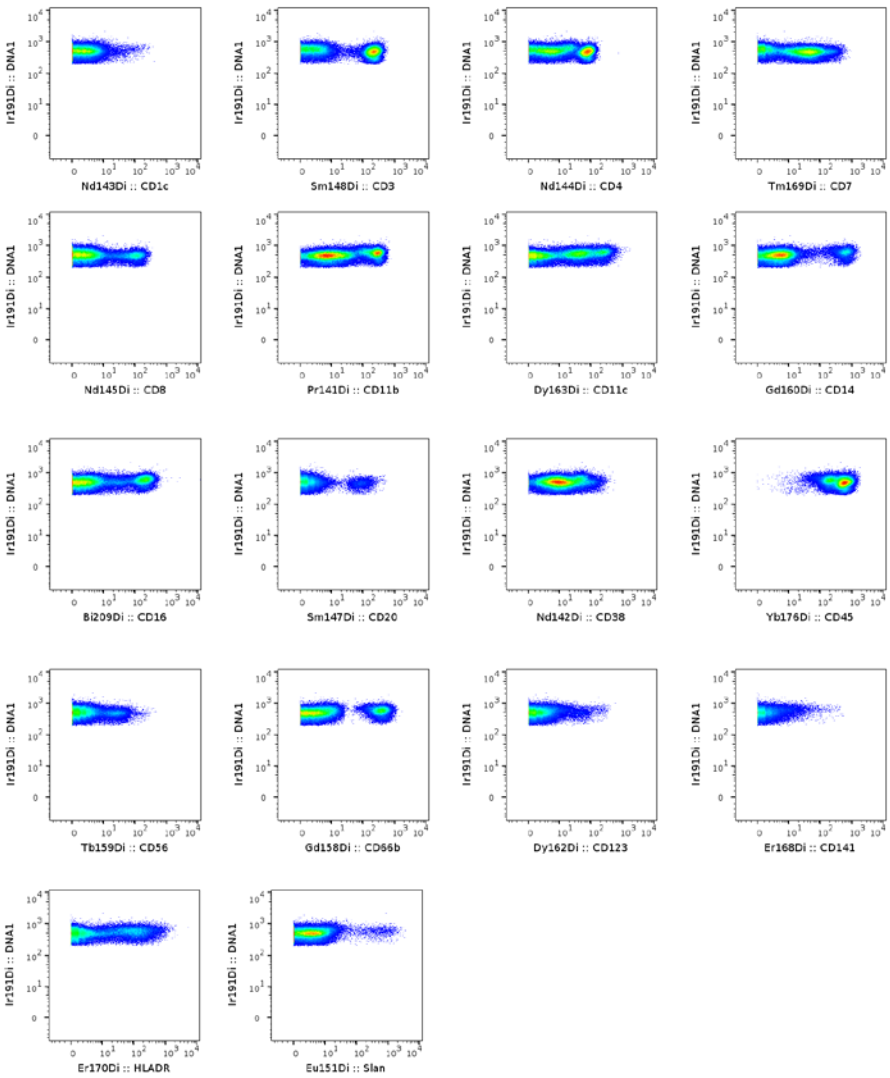

Fig. S2. Staining pattern in ungated cells. Staining patterns in ungated cells for all markers used for clustering

Fig. S3

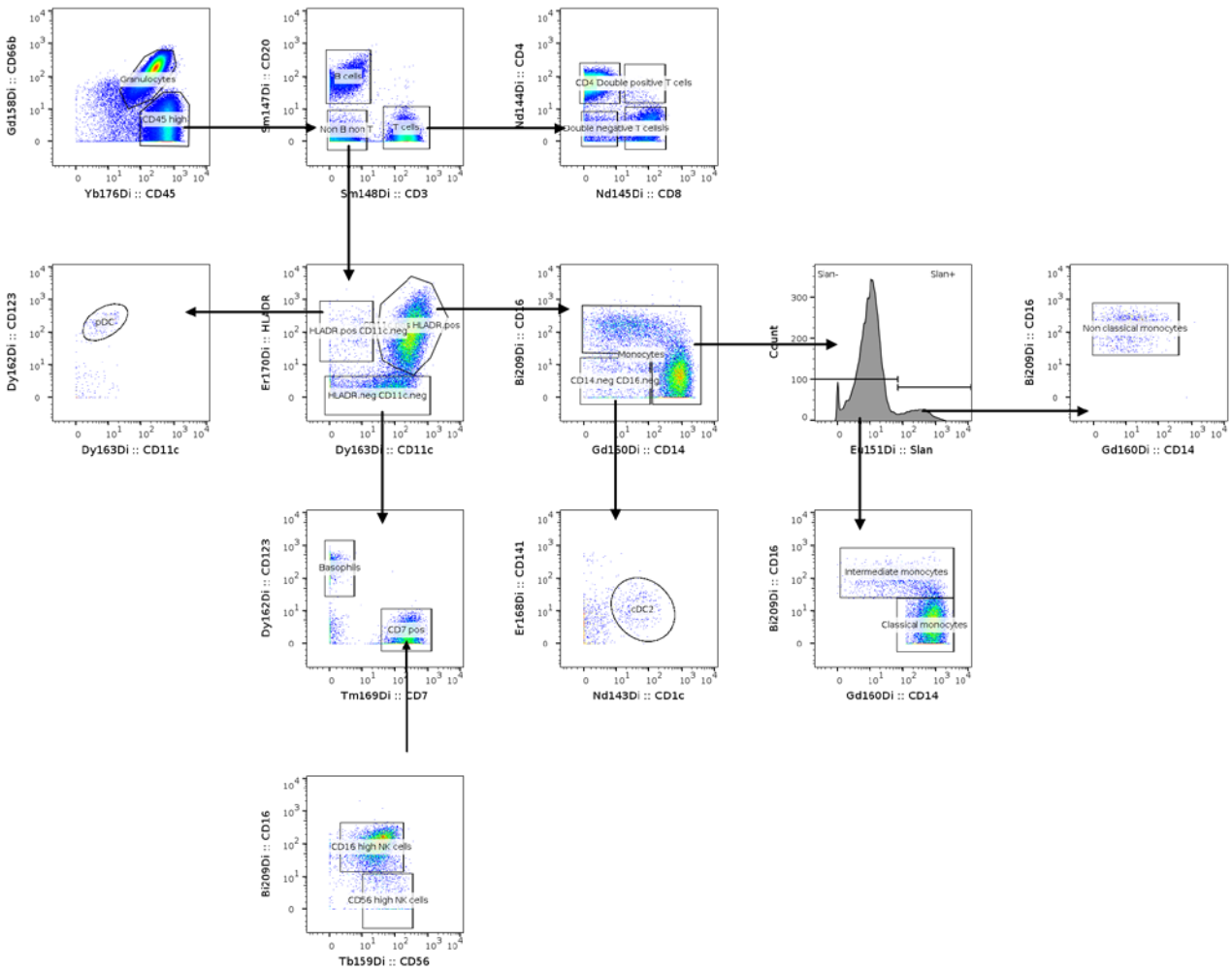

Fig. S3. Minimal gating example. Minimal gating example of a representative sample to illustrate marker expression in subsets.

Fig. S4

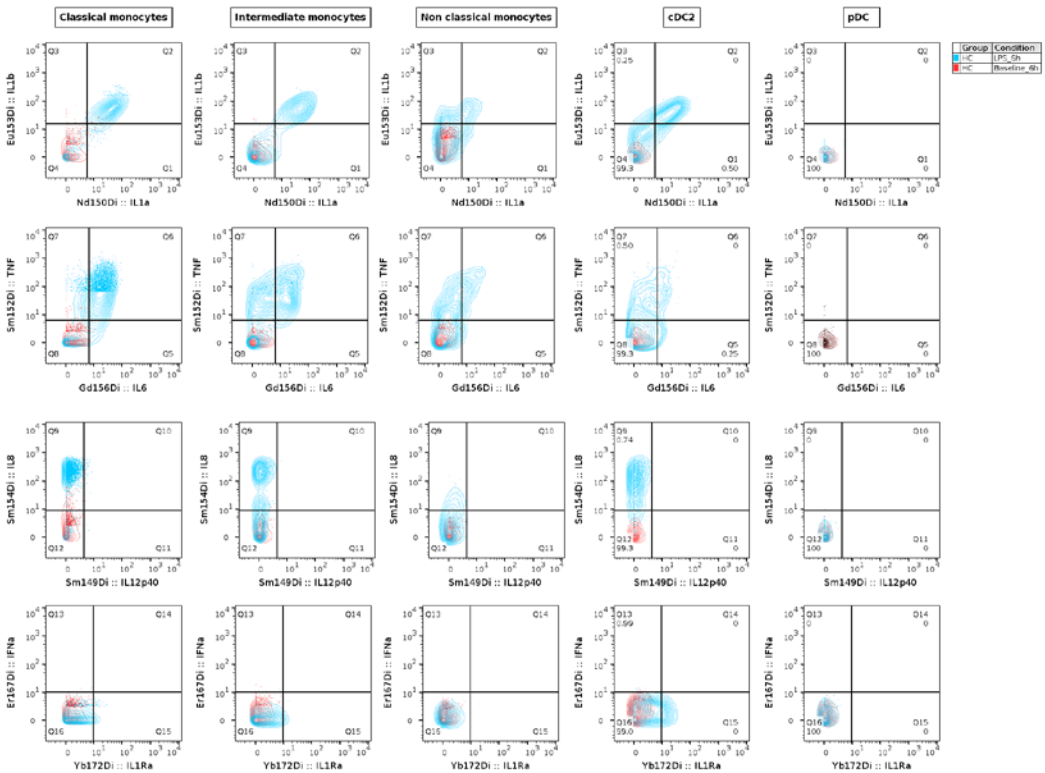

Fig. S4. Cytokine expression in healthy controls after LPS stimulation. Representative example of cytokine staining patterns in healthy controls in response to 6 h LPS stimulation. Red: unstimulated sample, blue: stimulated sample.

Fig. S5

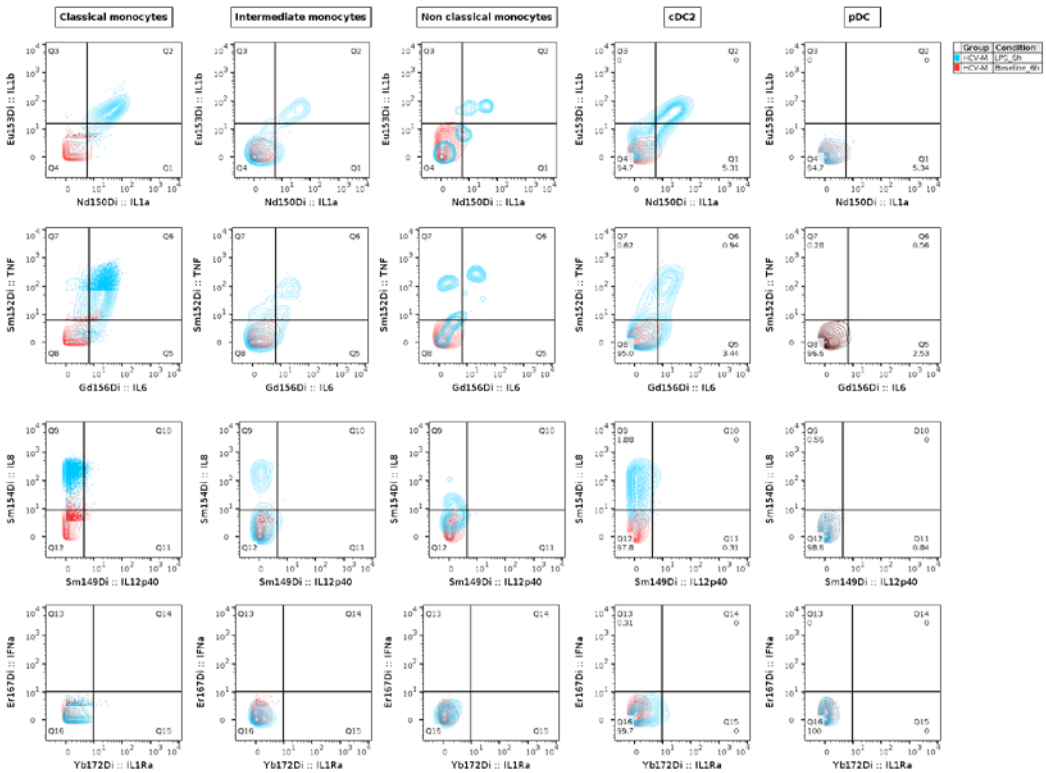

Fig. S5. Cytokine expression in HCV infected patients after LPS stimulation. Representative example of cytokine staining patterns in HCV infected patients in response to 6 h LPS stimulation. Red: unstimulated sample, blue: stimulated sample.

Fig. S6

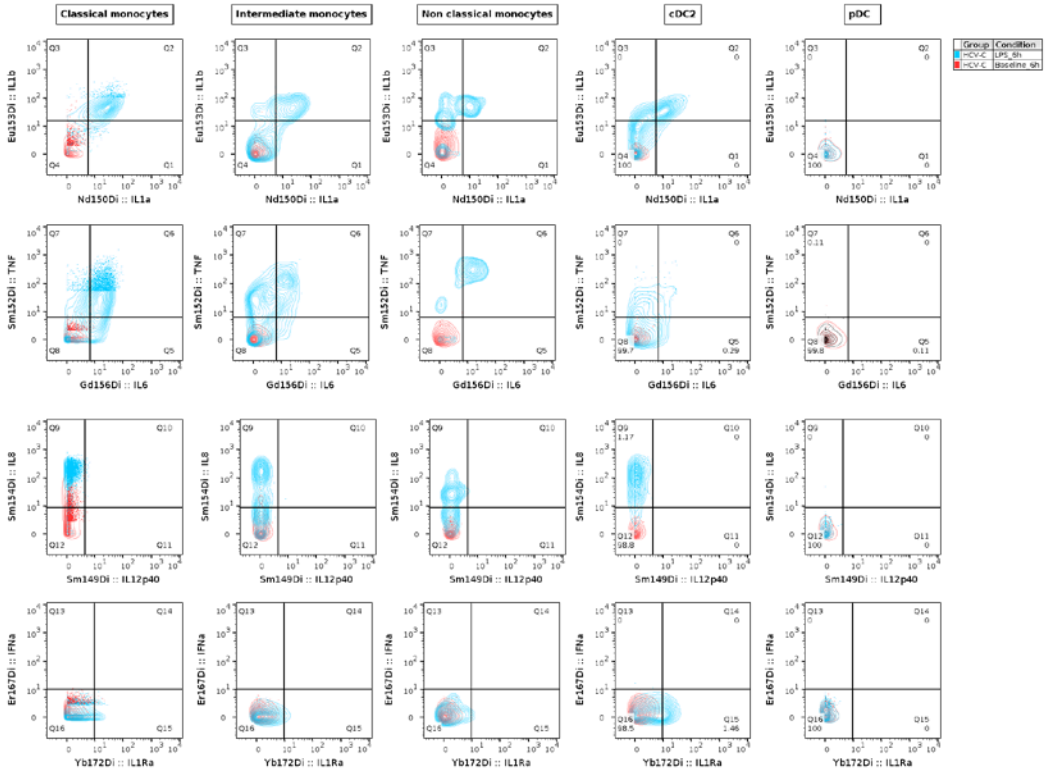

Fig. S6. Cytokine expression in HCV/HIV infected patients after LPS stimulation. Representative example of cytokine staining patterns in HCV/HIV infected patients in response to 6 h LPS stimulation. Red: unstimulated sample, blue: stimulated sample.

Fig. S7

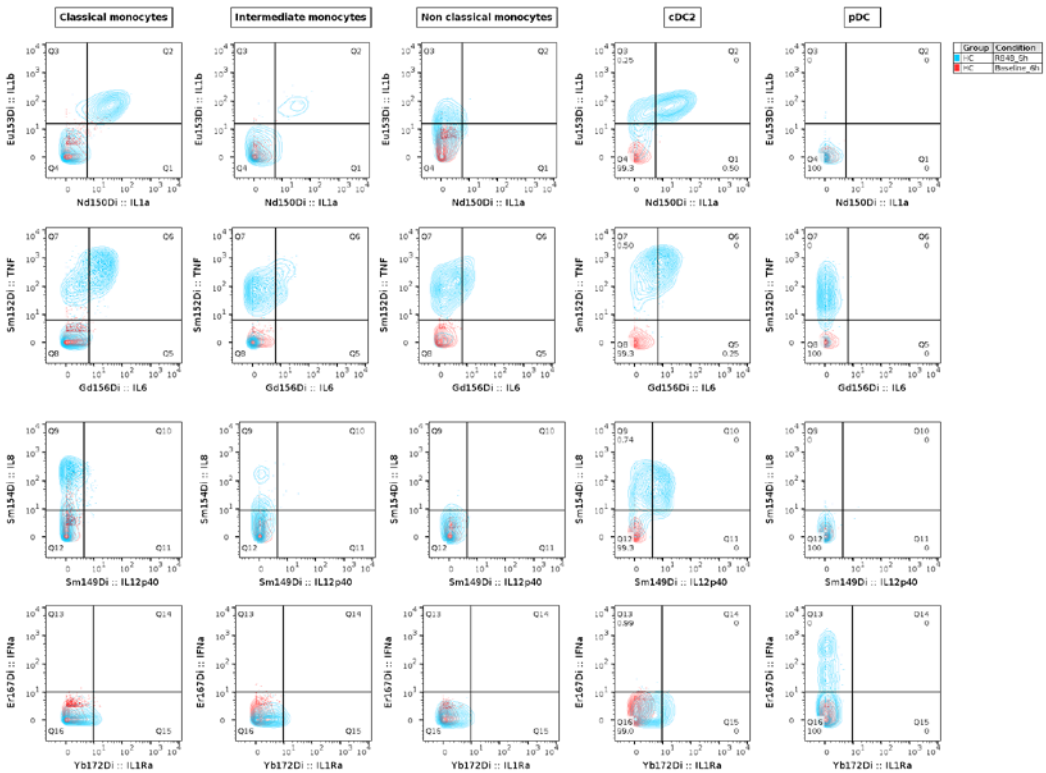

Fig. S7. Cytokine expression in healthy controls after R848stimulation. Representative example of cytokine staining patterns in healthy controls in response to 6 h R848 stimulation. Red: unstimulated sample, blue: stimulated sample.

Fig. S8

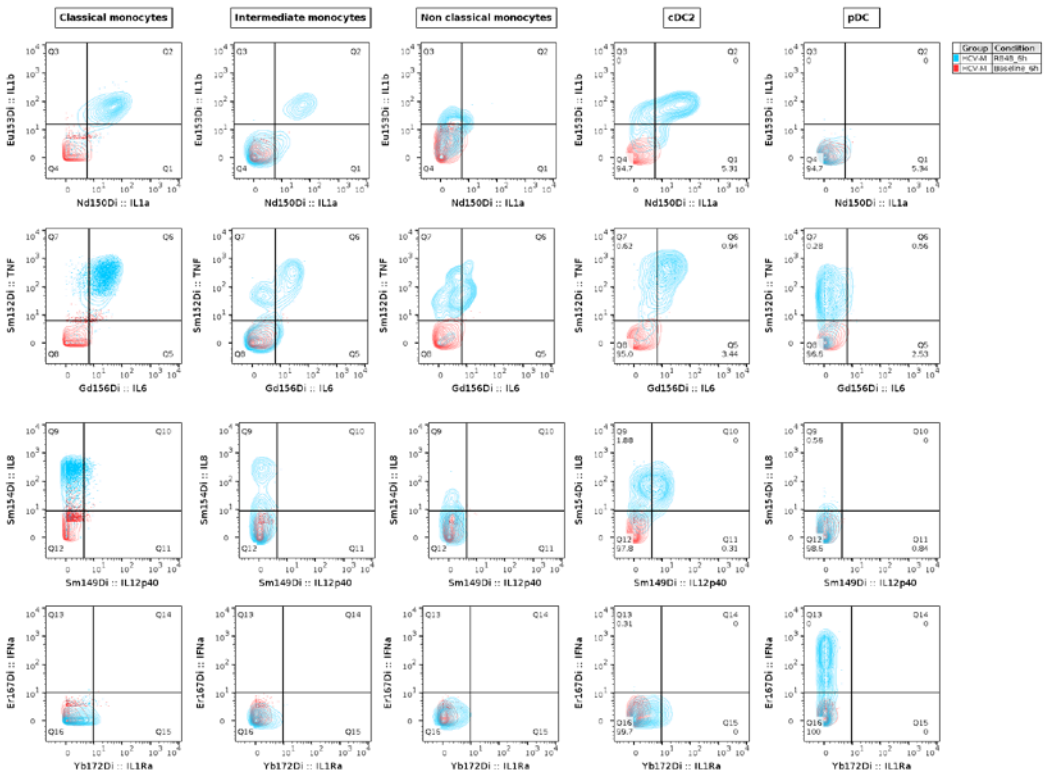

Fig. S8. Cytokine expression in HCV infected patients after R848stimulation. Representative example of cytokine staining patterns in HCV infected patients in response to 6 h R848 stimulation. Red: unstimulated sample, blue: stimulated sample.

Fig. S9

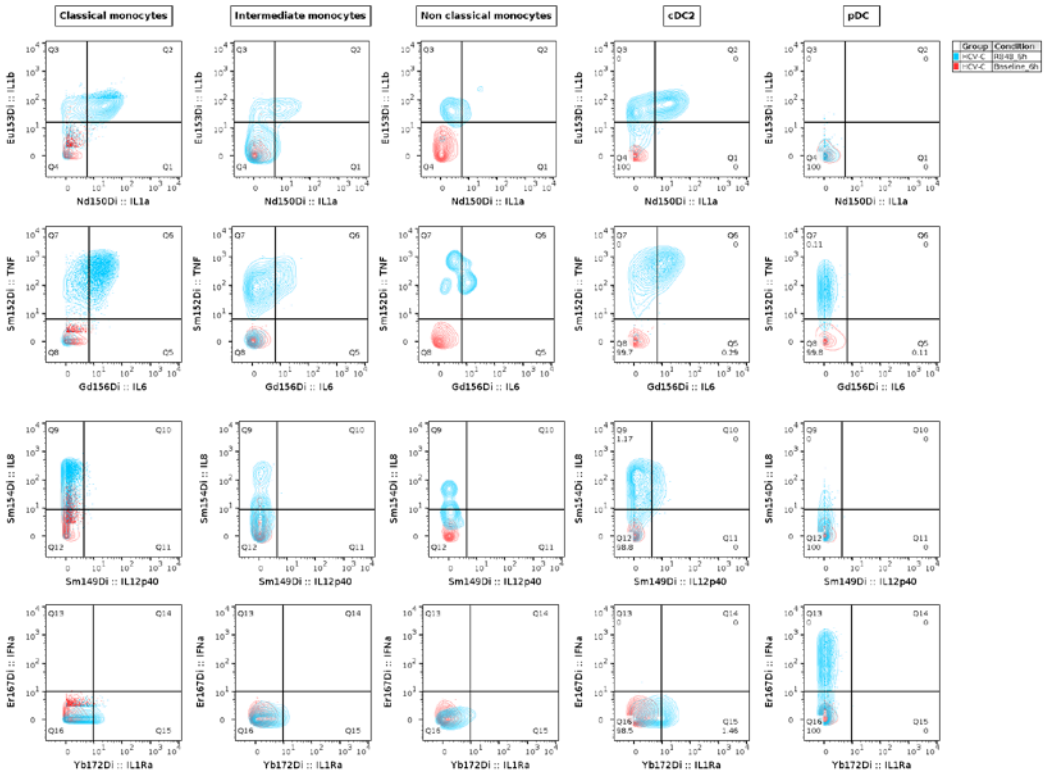

Fig. S9. Cytokine expression in HCV/HIV infected patients after R848stimulation. Representative example of cytokine staining patterns in HCV/HIV infected patients in response to 6 h R848 stimulation. Red: unstimulated sample, blue: stimulated sample.

Fig. S10

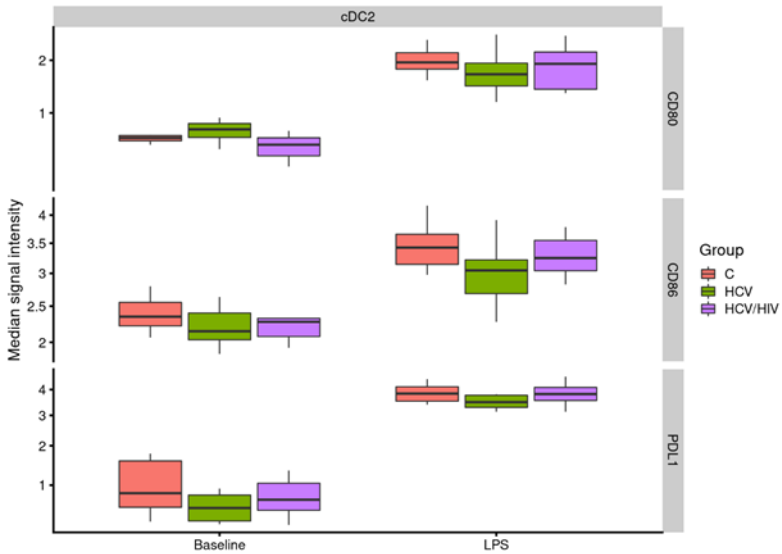

Fig. S10. Figure S9 Baseline and induced expression of inhibitory and co-stimulatory molecules in cDC2. Whole blood was stimulated for 24 h with 100 ng/mL of LPS. Left panels show baseline expression while right panel shows regulation in response to LPS..

Fig. S11

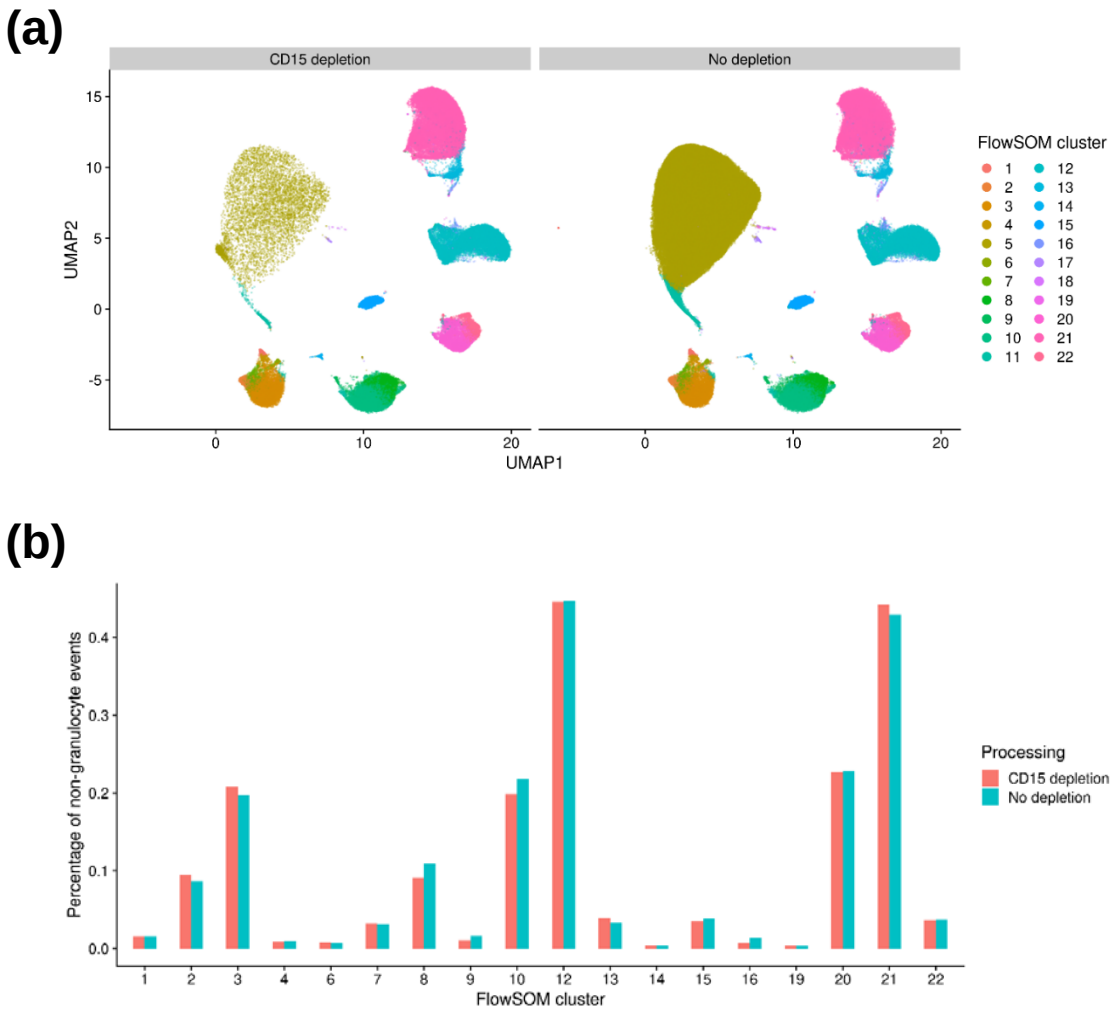

Fig. S11. Depletion of CD15 positive cells does not affect the frequency of other immune subsets. (a) UMAP plot of a split sample, granulocytes were depleted from half of the sample (left plot). (b) Frequencies of FlowSOM clusters with and without CD15 depletion. Frequency has been calculated as a percentage of non-granulocyte events and these clusters have been excluded from visualization. An independent FlowSOM run was used for this analysis.

High-dimensional immune phenotyping of blood cells by mass cytometry in patients infected with hepatitis C virus

Supplementary Materials and Methods

Blood stimulation and processing for CyTOF

We recruited 10 subjects in each study subgroup, without performing a power calculation as we did not have an accurate estimate of either variability between subjects nor of the immune response variability relative to antiviral treatment. All patients and volunteers were recruited by the Infectious Diseases Service (Prof Cavassini) with the exception of HCV mono-infected patients who were recruited by the Division of Gastroenterology and Hepatology (Prof Moradpour) of Lausanne University Hospital. Blood was collected in heparin tubes and either stabilized (see below) for frequency analysis or stimulated. Stimulation for cytokine expression was performed for 6 hours with 100 ng/mL *E. coli* O111:B4 Ultrapure LPS (Invivogen) or 5 µg/mL R848 (Invivogen) in the presence of 5 µg/mL brefeldin A (Biolegend). A 24-hour stimulation with LPS was used to investigate expression of co-stimulatory and inhibitory molecules. EDTA (2 mM, Merck) was added for the last 15 minutes of stimulation. Blood was stabilized using the Smart Tube Proteomic Stabilizer (Smart Tube Inc.). Briefly, 1.4 mL of Proteomic Stabilizer was added to 1 mL of blood and left to incubate for 10 minutes at 20°C to fix the cells. Samples were then stored at -80°C until processing, at which time they were thawed for 6 minutes in a 10°C water bath and red blood cells lysed twice for 5 minutes at 20°C in 25 mL of 1 x Lyse Buffer (Smart Tube Inc.). From each sample, 3 million cells were suspended in 1 mL of heat-inactivated FCS (Biochrom), passed through an 85-µm filter (Sefar, Nitex), washed three times in PBS, barcoded and stained.

Conjugation of antibodies for CyTOF analysis

Purified, carrier free, antibodies were purchased from Biolegend, BD, Miltenyi and Santa Cruz (Table S6) and conjugated using Multi-Metal Maxpar X8 kit. Conjugated antibodies were diluted to 0.2 mg/mL with antibody stabilizer and titrated over a range of 0.5 to 8 µg/mL.

Mass-tag barcoding

Palladium and indium isotopes were purchased from Trace Sciences and incorporated in isothiocyanobenzyl-EDTA (Scn-Bn-EDTA) and maleimido-mono-amide-DOTA (mDOTA) chelating agents [1, 2]. Barcode plates using titrated amounts of barcode reagents were prepared and stored at -80°C in zip-lock bags containing desiccant (Acros Organics). We used a hybrid barcoding strategy, consisting of a first barcoding step using a CD45-^{89}Y antibody, followed by incubation with Scn-Bn-EDTA and mDOTA barcode reagents [3]. Selected samples were incubated for 30 minutes with CD45-^{89}Y at RT and washed three times with ice-cold PBS before incubation with barcode reagents in 1 mL of PBS with 0.02% saponin for 30 minutes at 4°C. Scn-Bn-EDTA and mDOTA reagents were used at 200 nM and 400 nM. Barcode pools consisted of a balanced mix of samples to ensure presence of all stimulation conditions and multiple groups in each sample pool. Following barcoding, cells were washed three times with CSM and pooled in a 50 mL conical centrifuge tube (BD Falcon).

Sample staining and sample acquisition by CyTOF

To limit acquisition time, granulocytes were depleted using CD15-microbeads from 90% of each sample (Miltenyi) and an autoMACS Pro Separator (Miltenyi) according to the manufacturer's instructions. Depletion did not affect the frequency of other immune subpopulation (Figure S10). Samples were stained in 2 mL for 30 minutes at RT, washed and fixed overnight with 2% formaldehyde in PBS at 4°C. The following day, pooled samples were washed and incubated with antibodies against intracellular targets in CSM-S in a total volume of 2 mL for 30 minutes at 4°C. Pooled samples were washed and incubated with intercalation solution: PBS, 0.3% saponin, 1% formaldehyde, and 125 nM Iridium CellID (Fluidigm) for 30 minutes at RT before storing the sample at 4°C until acquisition. Samples were acquired as described [4]. Samples were washed twice with CSM and twice with miliQ before resuspension in 0.1X EQ beads (Fluidigm) and filtering through a 35 µm filter (BD Falcon). Samples were acquired on a daily tuned CyTOF 2 (upgraded from a CyTOF 1, Fluidigm) at an event rate of 300 cells/s using a syringe pump (New Era Pump Systems, Inc) set to 45 µL/min.

References

[1] Bodenmiller B, Zunder ER, Finck R, Chen TJ, Savig ES, Bruggner RV, et al. Multiplexed mass cytometry profiling of cellular states perturbed by small-molecule regulators. Nat Biotechnol 2012;30:858-867. 10.1038/nbt.2317

[2] Zunder ER, Finck R, Behbehani GK, Amir el AD, Krishnaswamy S, Gonzalez VD, et al. Palladium-based mass tag cell barcoding with a doublet-filtering scheme and single-cell deconvolution algorithm. Nat Protoc 2015;10:316-333. 10.1038/nprot.2015.020

[3] Behbehani GK, Thom C, Zunder ER, Finck R, Gaudilliere B, Fragiadakis GK, et al. Transient partial permeabilization with saponin enables cellular barcoding prior to surface marker staining. Cytometry A 2014;85:1011-1019. 10.1002/cyto.a.22573

[4] Ciarlo E, Heinonen T, Herderschee J, Fenwick C, Mombelli M, Le Roy D, et al. Impact of the microbial derived short chain fatty acid propionate on host susceptibility to bacterial and fungal infections in vivo. Sci Rep 2016;6:37944. 10.1038/srep37944

Table S1. Characteristics of patients and healthy subjects.

Group	Age	Sex	HCV genotype	METAVIR	HIV therapy	Year first HIV therapy	HCV therapy	CD4 count		HIV load		Sampling interval (weeks)
								Baseline	SVR12	Baseline	SVR12	
HCV	49	M	1	F3			EBR, GZR					25
	56	M	1	F4			LDV, SOF, RBV					41
	64	M	1	F2			LDV, SOF					27
	66	F	1	F3			LDV, SOF					25
	53	F	3	F4			DCV, SOF, RBV					39
	56	M	3	F3			DCV, SOF, RBV					29
	58	F	3	F2			DCV, SOF					26
	61	M	3	F4			DCV, SOF, RBV					31
	64	M	3	F4			DCV, SOF, RBV					25
	59	F	4	F2			EBR, GZR					26
HCV/HIV	37	M	1	F2	ABC, 3TC, ATV, RTV	1994	LDV, SOF	694	902	180	230	37
	38	M	1	F2	ABC, 3TC, DTG	1996	LDV, SOF	1083	1628	<20	<20	36
	50	F	1	F3	3TC, DRV, RTV, RAL	2005	LDV, SOF	644	997	<20	<20	24
	53	M	1	F4	FTC, TAF, DRV, RTV	1991	LDV, SOF	324	591	<20	<20	26
	55	M	1	F1	ZDV, 3TC, EFV	1998	LDV, SOF	546	663	<20	<20	25
	56	F	1	F1	ETV, DTG, DRV, RTV	2004	LDV, SOF	1297	1314	<20	<20	24
	59	M	1	F2	ABC, 3TC, ETV, RAL	1992	LDV, SOF	887	627	<20	<20	27
	54	M	3	F2	FTC, TAF, RPV	2012	DCV, SOF	287	431	<20	<20	24
	59	M	3	F1	EFV, TAF, FTC	2011	DCV, SOF	615	683	<20	<20	28
	58	M	4	F4	ABC, 3TC, DRV, RTV, DTG	2002	DSV, OBV, PTV, RTV, RBV	871	732	<20	<20	40
Controls	41	F										
	42	M										
	42	M										
	45	M										
	46	F										
	46	M										
	48	M										
	52	F										
	54	M										
	63	M										

Controls: healthy subjects. Antiviral therapy: 3TC: lamivudine, ABC: abacavir, ATV: atazanavir, COBI: cobicistat, DCV: daclatasvir, DRV: darunavir, DSV: dasabuvir, DTG: dolutegravir, EBR: elbasvir, EFV: efavirenz, ETV: etravirine, EVG: elvitegravir, FTC: emtricitabine, GZR: grazoprevir, LDV: ledipasvir, OBV: ombitasvir, PTV: paritaprevir, RAL: raltegravir, RBV: ribavirin, RPV: rilpivirine, RTV: ritonavir, SOF: sofosbuvir, TAF: tenofovir, ZDV: zidovudine. The HCV patients were significantly older than HCV-HIV patients ($p=0.042$) or healthy controls ($p=0.001$). The proportions of male and female were similar in patients and controls ($p=0.62$).

Table S2. Proportion of immune cell populations in the blood of healthy controls and HCV and HCV/HIV infected patients at baseline.

Population	Percent positive cells (median)			p value	
	Controls	HCV	HCV/HIV	HCV	HCV/HIV
cDC2	0.55	0.31	0.19	0.007	< 0.001
Intermediate monocytes	1.20	1.76	0.78		0.038
Non-classical monocytes	1.11	0.90	0.54		0.038
CD56 dim NK cells	8.08	4.72	3.61	0.074	0.012
B cells	4.58	4.99	9.80		0.125
CD11c positive B cells	0.14	0.24	0.42		0.042
CD4 T cells	41.00	43.80	29.80		< 0.001
Activated CD4 T cells	0.28	0.56	0.40	0.059	
CD8 T cells	16.70	20.10	23.40		< 0.001
Activated CD8 T cells	0.23	0.74	0.80	0.023	0.025
Activated DN T cells	0.07	0.10	0.19	0.042	< 0.001
Activated DP T cells	0.04	0.50	0.03	0.004	

Data are median percentage values of 10 controls or patients per group. Cell populations have been selected based on a p value ≤ 0.15 when compared to healthy controls. Statistical analysis of population abundance was performed using mixed linear models. Reported p values have been corrected for multiple testing using the false discovery rate.

Table S3. Proportion of immune cell populations in the blood of healthy controls and HCV and HCV/HIV infected patients at SVR12.

Population	Percent positive cells (median)			p value	
	Controls	HCV	HCV/HIV	HCV	HCV/HIV
cDC2	0.55	0.35	0.28		0.041
Intermediate monocytes	1.20	2.39	0.93	0.076	0.126
Non-classical monocytes	1.11	0.65	0.44		0.019
CD56 dim NK cells	8.08	4.53	3.56	0.146	0.02
CD56 high NK cells	0.43	0.25	0.26		0.088
B cells	4.58	3.80	8.47		0.061
CD11c pos B cells	0.14	0.20	0.27		0.146
CD4 T cells	41.00	44.60	33.70		0.015
Activated CD4 T cells	0.28	0.57	0.30	0.008	
CD8 T cells	16.70	18.00	25.20		0.001
Activated CD8 T cells	0.23	0.69	0.42	0.024	0.078
DN T cells	0.68	0.55	0.42		0.146
Activated DP T cells	0.04	0.45	0.04	0.002	

Data are median percentage values of 10 controls or patients per group. Cell populations have been selected based on p value ≤ 0.15 (highlighted in grey) when compared to healthy controls. Statistical analysis of population abundance was performed using mixed linear models. Reported p values have been corrected for multiple testing using the false discovery rate.

Table S4. Cytokine expression by TLR ligand-stimulated innate immune blood cells isolated from healthy controls and from HCV and HCV/HIV infected patients (baseline).

Population	Stimulus	Cytokine	Percent positive cells (median)			p value	
			Controls	HCV	HCV/HIV	HCV	HCV/HIV
Classical monocytes	LPS	IL-1α	89.6	84.7	88.4	0.149	
Classical monocytes	LPS	IL-1β	92.8	93.9	94.9		0.004
Classical monocytes	LPS	IL-8	89.8	94.1	92.1		0.125
Intermediate monocytes	LPS	IL-1β	90.8	94.4	91.1	0.071	
Intermediate monocytes	LPS	IL-8	68.0	81.4	73.1	0.007	
Non-classical monocytes	LPS	IL-1α	49.1	41.9	39.5		
Non-classical monocytes	LPS	IL-8	35.8	51.9	45.5	0.059	
Non-classical monocytes	LPS	TNF	86.8	92.7	95.2		0.045
cDC2	LPS	IL-1β	67.1	72.0	66.6		
Classical monocytes	R848	IL-1α	61.1	74.6	80.9		< 0.001
Classical monocytes	R848	IL-1β	66.4	83.8	91.0	0.041	< 0.001
Classical monocytes	R848	IL-6	46.3	46.1	70.4		< 0.001
Classical monocytes	R848	IL-8	48.2	69.9	68.5	0.016	0.004
Classical monocytes	R848	TNF	90.2	94.5	97.9		< 0.001
Intermediate monocytes	R848	IL-1α	39.2	58.6	51.0	0.002	0.038
Intermediate monocytes	R848	IL-1β	82.6	87.3	91.7		0.101
Intermediate monocytes	R848	IL-6	44.3	40.3	48.1		
Intermediate monocytes	R848	IL-8	23.3	50.7	37.5	0.001	0.021
Intermediate monocytes	R848	TNF	97.5	97.0	98.6		0.041
Non-classical monocytes	R848	IL-6	27.2	17.3	29.8		0.141
Non-classical monocytes	R848	TNF	96.1	95.6	97.7		0.049
cDC2	R848	IL-1α	47.7	48.2	60.3		0.031
cDC2	R848	IL-6	40.9	23.9	54.2		0.021
cDC2	R848	IL-12p40	61.8	46.1	49.1		0.026
cDC2	R848	TNF	98.7	96.1	97.7	0.023	0.005
pDCs	R848	IL-8	13.0	10.1	14.1		
pDCs	R848	IFNα	62.5	71.0	75.2		0.026

Data are median percentage values of 10 controls or patients per group. Cells were stimulated with LPS or R848. Cell populations have been selected based on a p value ≤ 0.15 (highlighted in grey) when compared to healthy controls. Statistical analysis of cytokine expression was performed using mixed linear models. Reported p values have been corrected for multiple testing using the false discovery rate.

Table S5. Cytokine expression by TLR ligand-stimulated innate immune blood cells isolated from healthy controls and from HCV and HCV/HIV infected patients (SVR12).

Population	Stimulus	Cytokine	Percent positive cells (median)			p value	
			Controls	HCV	HCV/HIV	HCV	HCV/HIV
Classical monocytes	LPS	IL-1α	89.6	85.0	92.0	0.015	
Classical monocytes	LPS	IL-1β	92.8	92.7	94.9		0.005
Classical monocytes	LPS	IL-8	89.8	93.0	94.3		0.005
Classical monocytes	LPS	TNF	89.7	77.9	84.2	0.029	0.091
Intermediate monocytes	LPS	IL-8	68.0	85.0	76.2	0.055	
Non-classical monocytes	LPS	IL-8	35.8	59.2	50.8	0.011	0.143
cDC2	LPS	IL-8	81.2	77.8	85.2		0.129
Classical monocytes	R848	IL-1α	61.1	61.8	75.2		0.001
Classical monocytes	R848	IL-1β	66.4	77.3	85.0		< 0.001
Classical monocytes	R848	IL-6	46.3	38.8	62.5		0.002
Classical monocytes	R848	IL-8	48.2	58.3	70.4	0.098	< 0.001
Classical monocytes	R848	TNF	90.2	90.0	95.8		< 0.001
Intermediate monocytes	R848	IL-1α	39.2	54.5	56.0		0.005
Intermediate monocytes	R848	IL-1β	82.6	86.6	89.9		0.143
Intermediate monocytes	R848	IL-8	23.3	47.5	32.5	0.100	0.016
cDC2	R848	IL-1α	47.7	43.6	63.5	0.143	0.026
cDC2	R848	IL-1β	95.2	91.3	96.7	0.043	
cDC2	R848	IL-6	40.9	16.8	51.4	0.133	0.100
cDC2	R848	TNF	98.7	97.0	98.1	0.100	

Data are median percentage values of 10 controls or patients per group. Cells were stimulated with LPS or R848. Cell populations have been selected based on a p value ≤ 0.15 when compared to healthy controls. Statistical analysis of cytokine expression was performed using mixed linear models. Reported p values have been corrected for multiple testing using the false discovery rate.

Table S6. Reagents.

Product	Manufacturer	Reference
Antibody Stabilizer PBS	Candor Bioscience	131 050
Bovine Serum Albumin	Sigma	A7906
Brefeldin A	Biolegend	420601
EDTA	Merck	E7889
Fetal calf serum (FCS)	Biochrom	S 0615
Formaldehyde	Thermo Scientific	28908
Human Immunoglobulin	CSL Behring	Beriglobin
Iridium cell-ID	Fluidigm	201192B
Isothiocyanobenzyl-EDTA	Dojindo	M030-10
E. coli O111:B4 Ultrapure LPS	Invivogen	trlr-3pelps
Mmaleimido-mono-amide-DOTA	Macrocyclics	B-272
MaxPar X8 conjugation kit	Fluidigm	201300
PBS	Bichsel AG	PBS-CHUV
Protein Stabilizer and Lysis buffer I	Smart Tube Inc.	PROT1
R848	Invivogen	tlrl-r848-5
Saponin	Sigma	84510
Sodium azide	Sigma	71289

Table S7. Antibodies and barcodes.

Target	Clone	Manufacturer	Isotope	Used for clustering
Barcode (CD45)	*HI30*	Fluidigm	*89Y*	
Barcode	*Scn-BN-EDTA*		*104Pd*	
Barcode	*Scn-BN-EDTA*		*105Pd*	
Barcode	*Scn-BN-EDTA*		*106Pd*	
Barcode	*Scn-BN-EDTA*		*108Pd*	
Barcode	*Scn-BN-EDTA*		*110Pd*	
Barcode	*mDOTA*		*113In*	
Barcode	*mDOTA*		*115In*	
CD1c	L161	Biolegend	143Nd	Yes
CD3	UCHT1	Biolegend	148Nd	Yes
CD4	RPA-T4	Biolegend	144Nd	Yes
CD7	CD7-6B7	Biolegend	169Tm	Yes
CD8	SK1	Biolegend	145Nd	Yes
CD11b	ICRF44	Biolegend	141Pr	Yes
CD11c	Bu15	Biolegend	163Dy	Yes
CD14	HCD14	Biolegend	160Gd	Yes
CD16	3G8	Fluidigm	209Bi	Yes
CD20	2H7	Biolegend	147Sm	Yes
CD38	HIT2	Biolegend	142Nd	Yes
CD45	HI30	Biolegend	176Yb	
CD56	R19-760	BD	158Gd	Yes
CD66b	REA306	Miltenyi	158Gd	Yes
CD80	2D10	Biolegend	161Dy	
CD86	IT2.2	Biolegend	146Nd	
CD123	6H6	Biolegend	162Dy	Yes
CD141	M80	Biolegend	168Er	Yes
HLA-DR	L243	Biolegend	170Er	
IFNα	LT27:295	Miltenyi	167Er	
IFNγ	B27	Biolegend	165Ho	
IL-1α	364-3B3-14	Biolegend	150Nd	
IL-1β	AS10	BD	153Eu	
IL-1Ra	AS17	SantaCruz	172Yb	
IL-6	MQ2-13A5	Biolegend	156Gd	
IL-8	BH0814	Biolegend	154Sm	
IL-10	JES3-12G8	Biolegend	175Lu	
IL-12-p40	C11.5	Biolegend	149Sm	
MCP-1	2H5	Biolegend	174Yb	
PD1	EH12.2H7	Biolegend	164Dy	
PD-L1	29E.2A3	Biolegend	171Yb	
Slan	DD1	Miltenyi	151Eu	Yes
TNF	Mab11	Biolegend	152Sm	

Table S8. Softwares.

Software name	Manufacturer	Version
Flowjo	FlowJo, LLC	10.2
MATLAB	Mathworks	R2014a
MATLAB Normalizer	Fink et al.	v0.3
R	R Foundation for Statistical Computing	3.4.2
Bioconductor	Bioconductor	3.6
ConsensusClusterPlus	Wilkerson & Hayes	1.42.0
cowplot	Wilke	0.9.2
data.table	Dowle & Srinivasan	1.10.4-3
flowCore	Ellis et al.	1.44.1
FlowSOM	van Gassen et al.	1.10.0
flowWorkspace	Finak & Jiang	3.26.4
fst	Klik	0.8.2
ggplot2	Wickham	2.2.1
lme4	Bates et al.	1.1-15
MASS	Venables & Ripley	7.3-48
Matrix	Bates & Maechler	1.2-12
multcomp	Hothorn et al.	1.4-8
mvtnorm	Genz et al.	1.0-6
ncdfFlow	Jiang et al.	2.24.0
openCyto	Finak et al.	1.16.1
pheatmap	Kolde	1.0.8
RcppArmadillo	Eddelbuettel & Sanderson	0.8.300.1.0
readxl	Wickham & Brian	1.0.0
Rtsne	Krijthe	0.14
scales	Wickham	0.5.0
stringr	Wickham	1.2.0
viridis	Garnier	0.4.1
Python	Python Software Foundation	3.7.7
Pandas	The pandas development team	1.0.3
UMAP	McInnes et al.	0.4.6

Legends of supplementary Figures

Fig. S1. Analyses of blood cell populations with mass cytometry. Blood samples were analyzed as described in Materials and Methods. UMAP plots show normalized signal intensity of markers used for clustering.

Fig. S2. Staining pattern in ungated cells. Staining patterns in ungated cells for all markers used for clustering

Fig. S3. Minimal gating example. Minimal gating example of a representative sample to illustrate marker expression in subsets.

Fig. S4. Cytokine expression in healthy controls after LPS stimulation. Representative example of cytokine staining patterns in healthy controls in response to 6 h LPS stimulation. Red: unstimulated sample, blue: stimulated sample.

Fig. S5. Cytokine expression in HCV infected patients after LPS stimulation. Representative example of cytokine staining patterns in HCV infected patients in response to 6 h LPS stimulation. Red: unstimulated sample, blue: stimulated sample.

Fig. S6. Cytokine expression in HCV/HIV infected patients after LPS stimulation. Representative example of cytokine staining patterns in HCV/HIV infected patients in response to 6 h LPS stimulation. Red: unstimulated sample, blue: stimulated sample.

Fig. S7. Cytokine expression in healthy controls after R848stimulation. Representative example of cytokine staining patterns in healthy controls in response to 6 h R848 stimulation. Red: unstimulated sample, blue: stimulated sample.

Fig. S8. Cytokine expression in HCV infected patients after R848stimulation. Representative example of cytokine staining patterns in HCV infected patients in response to 6 h R848 stimulation. Red: unstimulated sample, blue: stimulated sample.

Fig. S9. Cytokine expression in HCV/HIV infected patients after R848stimulation. Representative example of cytokine staining patterns in HCV/HIV infected patients in response to 6 h R848 stimulation. Red: unstimulated sample, blue: stimulated sample.

Fig. S10. Figure S9 Baseline and induced expression of inhibitory and co-stimulatory molecules in cDC2. Whole blood was stimulated for 24 h with 100 ng/mL of LPS. Left panels show baseline expression while right panel shows regulation in response to LPS..

Fig. S11. Depletion of CD15 positive cells does not affect the frequency of other immune subsets. (a) UMAP plot of a split sample, granulocytes were depleted from half of the sample (left plot). (b) Frequencies of FlowSOM clusters with and without CD15 depletion. Frequency has been calculated as a percentage of non-granulocyte events and these clusters have been excluded from visualization. An independent FlowSOM run was used for this analysis.